JOURNAL OF GEOPHYSICAL RESEARCH, VOL. 113, B08313, doi:10.1029/2007JB005418, 2008

Stress interaction effect on the occurrence probability of characteristic earthquakes in Central Apennines

R. Console,[1,2] M. Murru,[1] G. Falcone,[1,3] and F. Catalli[1]

Received 3 October 2007; revised 12 March 2008; accepted 29 April 2008; published 19 August 2008.

[1] In this study, we compute the effect of stress change due to previous historical earthquakes on the probability of occurrence of future earthquakes on neighboring faults. Following a methodology developed in the last decade, we start from the estimate of the probability of occurrence in the next 50 years for a characteristic earthquake on known seismogenic structures, based on a time-dependent renewal model. Then a physical model for the Coulomb stress change caused by previous earthquakes on these structures is applied. The influence of this stress change on the occurrence rate of characteristic earthquakes is computed, taking into account both permanent (clock advance) and temporary (rate-and-state) perturbations. We apply this method to the computation of earthquake hazard of the main seismogenic structures recognized in the Central and Southern Apennines region, for which both historical and paleoseismological data are available. This study provides the opportunity of reviewing the problems connected with the estimate of the parameters of a renewal model in case of characteristic earthquakes characterized by return times longer than the time spanned by the available catalogues and the applicability of the concept of characteristic earthquake itself. The results show that the estimated effect of earthquake interaction in this region is small compared with the uncertainties affecting the statistical model used for the basic time-dependent hazard assessment.

Citation: Console, R., M. Murru, G. Falcone, and F. Catalli (2008), Stress interaction effect on the occurrence probability of characteristic earthquakes in Central Apennines, *J. Geophys. Res.*, *113*, B08313, doi:10.1029/2007JB005418.

1. Introduction

[2] Seismic hazard in a given region can be assessed in a probabilistic way by the analysis of the effects, e.g. in terms of intensity (MMS) or peak ground acceleration (PGA), of past earthquakes in a suitably long time interval. The average recurrence time for exceedance of a given shaking level is computed on a grid of nodes covering the region, and the results can be shown in terms of contour maps at specific probability levels. Alternatively, the shaking level characterized by a given probability of exceedance in a specific time interval can be estimated and mapped, under a time-independent Poissonian model.

[3] A different and more physical approach to the probabilistic seismic hazard assessment (PSHA) pursues the estimate of the probability of rupturing of most (hopefully all) seismic sources in the concerned region for the time interval of interest. This approach can be applied either in a time-independent Poissonian hypothesis, or assuming a renewal model with memory. In the renewal model the elastic strain energy accumulates over a long period of time after the occurrence of one earthquake before the fault is prepared to release in the next earthquake. This model of earthquake occurrence assumes that the probability of an earthquake is initially low following a segment-rupturing earthquake, and increases gradually as tectonic processes reloads the fault. This probabilistic approach for forecasting the time of the next earthquake on a specific fault segment was initially proposed by *Utsu* [1972a, 1972b], *Rikitake* [1974] and *Hagiwara* [1974]. This model is typically associated with the hypothesis of characteristic earthquake, assuming that on a same seismogenic fault strong earthquakes occur with similar rupture areas, similar mechanisms, similar magnitudes and with time intervals characterized by remarkable regularity, but many other properties are sometimes associated with them [*Mc Cann et al.*, 1979; *Shimazaki and Nakata*, 1980, *Schwartz and Coppersmith*, 1984]. They are often assumed to have similar hypocenters, similar displacement distributions within the rupture area, similar source time functions (leading to similar seismograms), or quasiperiodic recurrence.

[4] The seismic gap model connected to this hypothesis assumes therefore that characteristic earthquakes are quasiperiodic with a characteristic recurrence time. According to the gap model, plate boundaries, like faults, are divided into segments, each with its own characteristic earthquake [*Fedotov*, 1968; *Mc Cann et al.*, 1979; *Nishenko*, 1989, 1991]. The faults tend to generate essentially the same size of the earthquake which has a relative narrow range of

[1] Istituto Nazionale di Geofisica e Vulcanologia, Rome, Italy.
[2] Centro di Geomorfologia Integrata per l'Area del Mediterraneo, Potenza, Italy.
[3] Earth Science Department, Messina University, Messina, Italy.

0148-0227/08/2007JB005418$09.00

magnitude near the maximum. The amount of slip that occurred in paste earthquakes will occur also in future [*Schwartz and Coppersmith*, 1984]. A seismic gap, according to the model, is a fault or plate segment for which the time since the previous characteristic event is close to or exceeds the characteristic recurrence time. In many applications, some past earthquakes are assumed characteristic, and the average time between them is assumed to be the characteristic recurrence interval. The characteristic hypothesis, which implies a sequence of recognizably similar events, provides the logical basis for discussing recurrence. A direct implication of the characteristic earthquake hypothesis is that the occurrence of earthquakes on individual faults and fault segments does not follow a log linear frequency-magnitude relationship of the form (log N = a − bM) described by *Gutenberg and Richter* [1956]. The characteristic earthquakes are assumed large enough to dominate the seismic moment release and substantially reduce the average stress.

[5] This approach to earthquake forecasting has been widely applied, particularly in Japan and the United States, as a basis for long-term forecasts of future seismic activity. In Italy, a similar approach has been applied by *Boschi et al.* [1995]. The difference with the methodology followed in this study is that those authors compiled earthquake sequences by selecting earthquakes if their magnitude exceeded a given threshold, and if their epicenters belonged to specific seismic areas. No attention was paid to the association of those events to individual sources. The modest magnitude threshold adopted in their study (4.5) implied also relatively modest recurrence times in comparison with those dealt with in our study.

[6] It is commonly accepted that the regularity of characteristic earthquakes can be affected by interaction between neighboring faults, modifying the probability of occurrence of future events. The interaction may result in three possible ways: the occurrence of an earthquake is advanced or delayed, or the earthquake is triggered instantaneously [*Zöller and Hainzl*, 2007]. Positive interaction is a well known phenomenon: a large earthquake can change the static stress on surrounding faults up to distances of hundred kilometers promoting their rupture, and activating aftershock sequences. In several cases a clear correlation has been noted between the pattern of positive Coulomb stress change and the increase of the local occurrence rate density, both in normal and in strike fault systems [*King et al.*, 1994; *Harris and Simpson*, 1998; *King and Cocco*, 2001]. Focusing our attention on the geographical region considered in this study, a clear example of such correlation has been put in evidence by *Murru et al.* [2004] and *Nostro et al.* [2005], for the Colfiorito earthquake sequence that hit the Umbria-Marche Central Apennines from September 1997 up to April 1998. The correlation appeared significant for Coulomb stress changes larger than 0.02–0.1 MPa.

[7] According to the methodology developed in the last decade [*Stein et al.*, 1997; *Toda et al.*, 1998; *Parsons*, 2004], the probability of the next characteristic earthquake on a known seismogenic structure in a future time interval starts from the estimate of its occurrence rate, conditioned to the time elapsed since the previous event. To do it, two characteristic parameters are necessary: the expected recurrence time and the aperiodicity of the renewal process. Then, a physical model for the Coulomb stress change caused by previous earthquakes on this structure is applied. The influence of this stress change is computed by the introduction of a permanent shift on the time elapsed since the previous earthquake (clock advance), or by a modification of the expected recurrence time.

[8] A further perturbation to the probability can be introduced during a relatively short time following the previous events causing the stress change: this is represented by a non-linear dependence of the variation of seismic rate on the static stress change derived from the rate-and-state model for earthquake nucleation introduced by *Ruina* [1983] and *Dieterich* [1986, 1992, 1994]. This model has been included by *Console et al.* [2006, 2007] in a physical and stochastic epidemic-type algorithm for earthquake clustering. However, *Stein et al.* [1997], *Toda et al.* [1998], and *Parsons* [2004] have applied it also to estimate the probability of failure of single faults, even if this specific application still represents a controversial and discussed issue [*Gomberg et al.*, 2005a, 2005b].

[9] The present study should be regarded as of methodological nature. We want to test the applicability and the eventual limitations of the above mentioned methodology, and to assess the impact of different assumptions on the estimate of the probability of occurrence of major earthquakes in a well known seismogenic region. The application is made to a wide part of the Apennines chain included in the rectangle of coordinates 40°–43°N and 13°–17°E (Figure 1).

2. Method

[10] A standard procedure for seismic hazard assessment assumes that all relevant earthquakes occur on well recognized faults with characteristic mechanism and size. The procedure needs the adoption of a probability density function $f(t)$ (pdf) for the inter-event time between consecutive events on each fault, together with some basic parameters of the model. One can adopt either a time-independent Poisson model or a time-dependent renewal model. For the former model, the expected recurrence time T_r is the only necessary piece of information. For the latter, also a parameter as the coefficient of variation (also known as aperiodicity) α, defined as the ratio between the standard deviation and the average of the recurrence times, is required.

[11] Several other functions related to the pdf are commonly used in reliability applications. In the following some of the most important in seismic hazard studies are reviewed.

[12] The cumulative density function $F(t)$ (cdf) is the probability that the elapsed time T takes a value less or equal to t. That is (integrating over the recurrence time variable u, and taking into account that u cannot be negative):

$$F(t) = \Pr[T \le t] = \int_0^t f(u)du. \tag{1}$$

Its complement to 1, the survival function $S(t)$, is the probability that the elapsed time T takes a value greater than t:

$$S(t) = \Pr[T > t] = 1 - F(t). \tag{2}$$

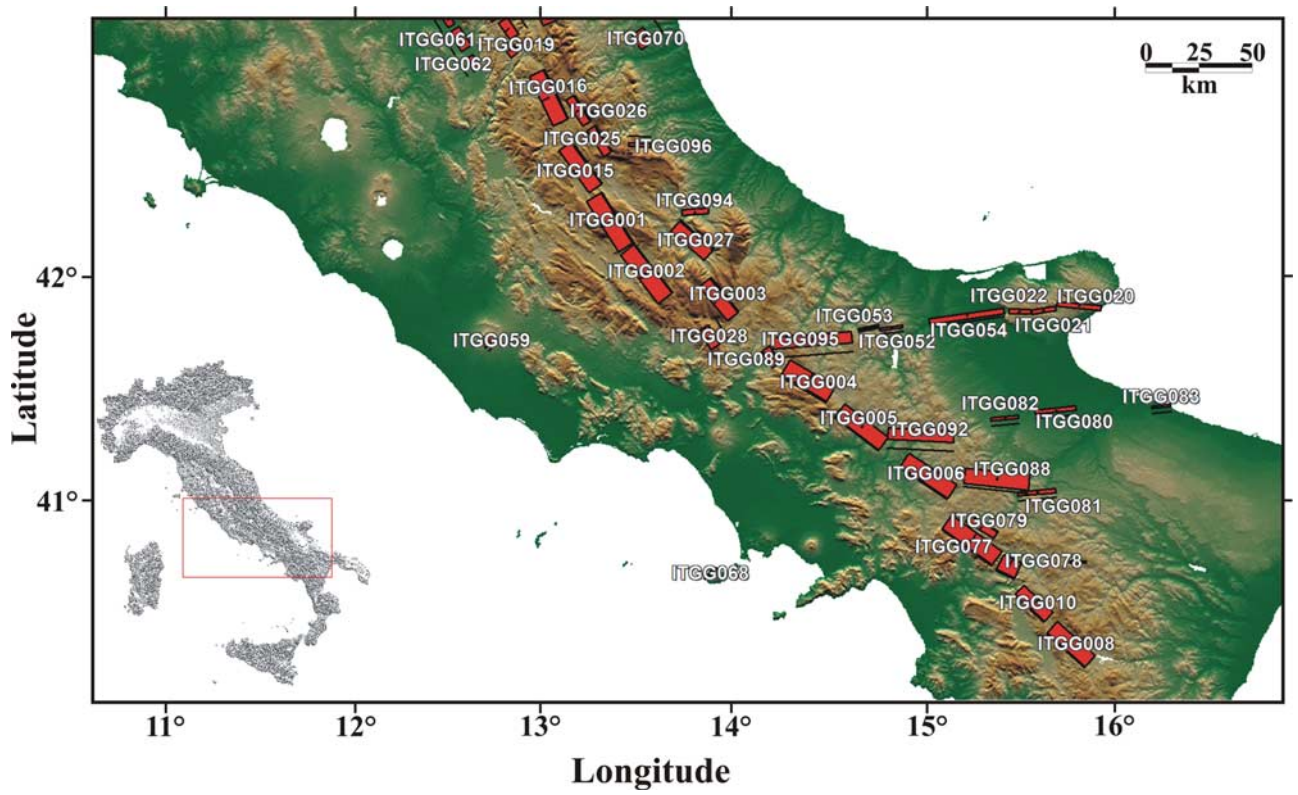

Figure 1. Map of the area in analysis, including 35 seismogenic sources (*database* DISS 3.0.2, September 2006).

The hazard function $h(t)$ is the ratio of the pdf $f(t)$ to the survival function, $S(t)$:

$$h(t) = \frac{f(t)}{S(t)} = \frac{f(t)}{1 - F(t)}. \tag{3}$$

Integrating the hazard function for a constant $S(t)$ we obtain the cumulative hazard function $H(t)$, which can be interpreted as the probability that the variable T takes values greater than t and less than $t + \Delta t$, conditioned to the fact that T is greater than t:

$$H(t < T \le t + \Delta t) = \Pr[t < T \le t + \Delta t | \mathrm{T} > \mathrm{t}] = \frac{\Pr[t < T \le t + \Delta t]}{\Pr[t < T]} = \frac{\int_t^{t+\Delta t} f(u)du}{S(t)}. \tag{4}$$

There are various types of probability distributions used as models for stationary-point processes and adopted in the works published in seismological literature. *Stein et al.* [1997] assumed a classical log normal distribution, *Toda et al.* [1998] assumed a Weibull distribution, while *Parsons* [2004] and *Pace et al.* [2006] preferred the Brownian Passage Time (BPT) distribution introduced by *Kagan and Knopoff* [1987] and successively described in detail by *Ellsworth et al.* [1999] and *Matthews et al.* [2002]. The differences in pdf and cdf among these statistical models are minor, although the differences in the hazard function for large recurrence times may be substantial [*Matthews et al.*, 2002]. In lack of observational evidence, in this study we adopt the BPT to represent the recurrence time probability distribution for earthquakes on single sources in Italy. This distribution is expressed as

$$f(t; T_r, \alpha) = \left(\frac{T_r}{2\pi\alpha^2 t^3}\right)^{1/2} \exp\left\{-\frac{(t - T_r)^2}{2T_r\alpha^2 t}\right\}, \tag{5}$$

with the previously given meaning of T_r and α.

[13] The cdf for the BPT can be expressed in terms of the cumulative Gaussian probability function (also known as erf); however, in this study we adopt a method of numerical integration by discretization. By substitution of equation (5) into (4) we may obtain the probability that an event occurs between time t and $t + \Delta t$, under the condition that no other event has occurred after time $t = 0$ (i.e., after the occurrence time of the last characteristic event).

[14] *Zöller and Hainzl* [2007] describe the BPT model as a purely periodic "stick-slip" motion decorated with a stochastic Brownian walk accounting for subscale processes. Events like small earthquakes, aseismic stress release, spatial etherogeneities, or pore pressure changes could be the causes of such minor perturbations. Therefore this model assumes that earthquakes occur on isolated faults, without taking into account major interactions between neighboring faults.

[15] As stated in the introduction, it is supposed that in real circumstances earthquake sources may interact, so that earthquake probability may be either increased or decreased with respect to what would be expected by a simple renewal model. The interaction is taken into consideration by the computation of the Coulomb static stress change, also known

as the Coulomb Failure Function (ΔCFF), caused by previous earthquakes on the concerned fault [*King et al.*, 1994]:

$$\Delta CFF = \Delta\tau + \mu'\Delta\sigma_n, \tag{6}$$

where $\Delta\tau$ is the shear stress change on a given fault plane (positive in the direction of fault slip), $\Delta\sigma_n$ is the fault-normal stress change (positive when unclamped), and μ' is the effective coefficient of friction [*King and Cocco*, 2001].

[16] For this computation, the knowledge of the fault parameters (strike, dip, rake, dimensions, and average slip) is necessary for all the triggering earthquakes. An assumption for the earthquake mechanism of the triggered source is also needed. Dealing with old events, for which details as fault shape and slip heterogeneity are not known, we assume rectangular faults with uniform slip distribution. The algorithm for ΔCFF computation assumes an Earth model such as a half-space characterized by uniform elastic parameters. As ΔCFF is strongly variable in space, we consider its value in the point of the triggered fault where it may have the largest effect.

[17] As recalled in the introduction, the effect of ΔCFF on the probability for the future characteristic event through equation (4) can be considered from two viewpoints [*Stein et al.*, 1997; *Parsons*, 2005]. The first view point assumes that the time elapsed since the previous earthquake is modified from t to t' by a shift proportional to ΔCFF, that is

$$t' = t + \frac{\Delta CFF}{\dot{\tau}} \tag{7}$$

where $\dot{\tau}$ is the tectonic stressing rate, supposed unchanged by the stress perturbation.

[18] The second view point works on the idea that the stress change can be equivalent to a modification of the expected recurrence time T_r:

$$T_r' = T_r - \frac{\Delta CFF}{\dot{\tau}}. \tag{8}$$

Note that the minus sign in equation (8) corrects the plus sign on the equivalent expression by *Parsons* [2005, page 12]. According to *Stein et al.* [1997] both methods yield similar results. However, in our experience, they lead to different results, in particular when the elapsed time t is significantly smaller or larger than the recurrence time T_r, and also when the time interval Δt is not negligible with respect to T_r.

[19] *Parsons* [2005, Figure 15] showed the difference in using the two different approaches, i.e., the elapsed time shift (clock change) (equation (7)) and the inter-event time change (equation (8)) for the interaction between the 1906 San Francisco earthquake and the north Hayward fault. The two methods generate different probability values at different times in the earthquake cycle. There is no clear justification for choosing one method over the other, and the differences must be considered as part of the variability associated with interaction probability calculations. In our applications, the choice between the first and the second view has been decided in favor of the first one, under the consideration that the second view has the consequence of producing an asymptotic change of the recurrence time [*Parsons*, 2005].

[20] Equations (7) and (8) express what has been called "permanent effect" of the stress change by *Stein et al.* [1997]. We then need to consider also the so-called "transient effect," due to rheological properties of the slipping faults. The application of the *Dieterich*'s [1994] constitutive friction law to an infinite population of faults (imagined as characterized by a complete distribution of states) leads to the expression of the seismicity rate as a function of time after a sudden stress change:

$$R(t) = \frac{R_0}{\left[\exp\left(\frac{-\Delta CFF}{A\sigma}\right) - 1\right]\exp\left(-\frac{t}{t_a}\right) + 1} \tag{9}$$

where R_0 is the seismicity rate before the stress change, A is a fault constitutive parameter, σ is the normal stress acting on the fault, t_a is a time constant equal to $A\sigma/\dot{\tau}$, and $\dot{\tau}$ is the tectonic stressing rate (supposed unchanged by the stress step). The simplified relationship between $A - \sigma$ and stressing rate is only valid during the self-accelerating rate-state time history [*Dieterich*, 1994].

[21] Here and in the following of this article, all the seismicity rates are defined as the number of earthquakes of magnitude exceeding a given threshold m_0, per unit time and area.

[22] In all our applications of equation (9), $A\sigma$ works as a single parameter. Its value can be determined by experimental observations on real seismicity, rather than being derived from assumptions on A and σ separately. It can be easily recognized that the time-dependent rate $R(t)$ tends to R_0 when time goes to infinity.

[23] We apply equation (9) to individual faults, with the substitution of the appropriate value for the hazard rate in place of the background rate R_0. For this computation we assume a constant hazard rate, although the conditional probability obtained for the BPT increases with elapsed time, in consideration of the fact that the time constant T_r (typically hundreds to thousands of years) is much larger than t_a (typically few years) [*Stein et al.*, 1997].

[24] It may appear unjustified to apply equation (9), originally derived from statistical considerations on an ideal infinite population of faults [*Dieterich*, 1994], to a single fault the state of which should be deterministically linked to the time elapsed since the previous failure [*Gomberg et al.*, 2005a, 2005b]. The idea is considering a fault plane as an infinite array of nucleation patches.

[25] The justification may be found in three ways:

[26] 1. The fault does not have a homogeneous distribution of stress and strength; each small area of its surface could represent a single sample of the ideal population for which equation (9) holds.

[27] 2. Even if the whole fault is retained as a single object characterized by a well identifiable state, it can be thought as a sample of as many ideal faults as we want; to this single object we may apply the statistical concepts described in equations (1) to (4) exactly in the same way as a single person might make use of statistical tools for estimating the convenience of signing a contract of insurance on his own life.

[28] 3. Geometric variations in fault structure (bends, steps, jogs) or material properties would lead to an array of varying nucleation conditions.

[29] Once the time-dependent rate $R(t)$ is estimated by equation (9), the expected number of events N over a given time interval $(t, t + \Delta t)$ is computed by integration:

$$N = \int_t^{t+\Delta t} R(t)dt. \tag{10}$$

Under the hypothesis of a generalized Poisson process, we may finally estimate the probability of occurrence for the earthquake in the given time interval:

$$P = 1 - \exp(-N). \tag{11}$$

3. The Data

[30] In this study we consider a wide region of the Apennines, limited by the rectangle of coordinates 40°–43°N and 13°–17°E (Figure 1). The implementation of the method outlined in the previous section requires quantitative information about the faults that may interact among each other. For this purpose we make use of the most comprehensive source of information available about Italian seismogenic sources: the Database of Individual Seismogenic Sources (DISS) owned by Istituto Nazionale di Geofisica e Vulcanologia [*DISS Working Group*, 2006]. A short outline of this source of information is given in the following section.

3.1. The Database of Italian Seismogenic Sources

[31] The first version of DISS is dated July 2000, and the most recent (version 3.0.3) has been released in 2007.

[32] DISS regards seismogenic sources as a simplified and georeferenced 3D representation of fault planes, identified through geological and geophysical investigations. They are supposed capable of primary slip during a strong earthquake and are assumed to exhibit ''characteristic'' behavior with respect to rupture length/width and expected magnitude. These sources are called Geological and Geophysical sources (GG). According to the authors of DISS, a characteristic behavior does not imply regularity for the occurrence of characteristic earthquakes. Rather then that, the authors claim that the word ''characteristic'' refers only to the shape, size and average slip of each main shock on the same fault. However, according to a simple and intuitive reasoning, it is unlikely that a seismic source that produces earthquakes characterized by quite the same shape, size and slip (and consequently the same magnitude and seismic moment) in a constant regional stress rate regime, doesn't have a regular inter-event time. The perturbations to this regularity due to the interaction among different sources are the subject of the present study.

[33] The DISS database contains also information about seismogenic sources that cannot be reliably assessed using geological and seismological data only. This information is derived from quantitative treatment of historical earthquake data. In this study we shall mainly focus on the first group of individual GG sources. For each of them, DISS stores, among others, the following parameters, estimated from various kinds of geological, geodetic, geomorphological and seismological data, or inferred from other parameters through empirical relationships [e.g., *Wells and Coppersmith*, 1994]:

[34] (1) location (lat/lon) of the center of the fault, (2) length and width of the fault, (3) minimum and maximum depth, (4) strike, dip and rake of the fault, (5) average slip, (6) slip rate (minimum and maximum), (7) recurrence time (minimum and maximum), (8) maximum magnitude (Mw), (9) date of the latest earthquake, and (10) date of penultimate earthquake (when available).

[35] It may be useful to recall that the DISS database does not deal with renewal models and the coefficient of variation α is not part of the database.

[36] We give in the following a short outline of the information available for some of the reported parameters, leaving the details about the criteria adopted in their compilation to the authors of the database [*DISS Working Group*, 2006]. In no way this study is aimed at revising the information stored in the DISS database, except for the comparison of such information with data derived from alternative sources, such that obtained from paleoseismological or recent geodetic observations.

[37] DISS 3.0.2 describes 109 Italian individual seismogenic sources (35 of which, whose location is known, fall in Figure 1). The magnitude associated to these sources ranges from 5.3 to 7.0. According to standard relationships [*Wells and Coppersmith*, 1994] these magnitudes are related respectively to a fault length of 5 km with a coseismic slip equal to 0.16 m, and to a fault length of the order of 35 km with a slip larger than 2 m. Therefore the individual sources identified by DISS 3.0.2 are characterized by a fairly wide range of sizes.

[38] For some of the seismogenic sources included in DISS the respective length (L), width (W), slip per event (D) and magnitude (M) are all known from independent observations. In this case the different estimations can be used alternately with the scaling relationships, and the consistency of a seismogenic source with some generalized model can be analyzed. Most likely, only one or two of these parameters are known with confidence and can then be used to determine the others. In case only M is known (e.g., the source is based on an instrumentally recorded earthquake), L, W, and D can be calculated from scaling relationships. Conversely, M can be estimated if one or more of the other parameters are known. When only one among L, W, or D is known and M is known, the compiler first verifies if they agree with one another, then determines the other parameters. If they do not agree, the compiler must choose the best constrained data through independent observations and all other parameters are based on it. This procedure guarantees that the characterization of seismogenic sources does not differ significantly from present knowledge of the earthquake process while preserving at least some seismologic and geologic observations [*Basili et al.*, 2008].

[39] The slip rate (mm/year) and the recurrence time (year) are the parameters with the largest degree of uncertainty for most of the sources reported in DISS 3.0.2. These two parameters are linked together for a single characteristic earthquake, i.e. slip rate = slip per event/recurrence interval. The slip rate can be determined in three ways: from the

Table 1. Chronology of the Events on the Faults for Which Paleoseismological Data are Available[a]

Source Code	ITGG001	ITGG002	ITGG003	ITGG077	ITGG096
Source Name	Ovindoli-Pezza	Fucino Basin	Aremogna	Irpinia (Colliano)	Isola del Gran Sasso
Event 1	700–3690	85	651–2800	20	800–5480
Event 2	3420–7620	1382–1492	4940–5735	1770–2620	7475–9155
Event 3	5460–20000	3100–3600	5366–7000	2620–4320	14120–31500
Event 4		4200–5944		4460–6790	
Event 5		6000–7979		6790–8650	
Event 6				11230–????	

[a]All times are given in years before present (2000AD).

displacement of dated geological markers, displacement observed through geodetic measurements and from displacement calculated from seismic or geodetic strain. Assuming that the slip of a characterisitic event is a fairly well constrained parameter, we may infer that the relative errors of the slip rate and of the recurrence time are approximately proportional to each other.

[40] Because of lack of reliable geodetic measurements of crustal strain in Italy, the slip rate is, in many cases, assumed to fall in the range 0.1–1.0 mm/year by geodynamic constraints. For little more than 20 sources, thanks to paleoseismological or geomorphological constraints, the slip rates and the recurrence times are known within a smaller range of variation. As the recurrence time T_r is one of the most critical parameters to be used in seismic hazard analysis, we have made a small statistical analysis of this parameter as reported by DISS 3.0.2. The minimum T_r ranges from 570 y to 2500 years, and its average is 902 ± 387 years. The maximum T_r ranges from 833 y to 25,000 years, and its average is 4,947 ± 3,782 years.

[41] The date of the latest earthquake is unknown for 13 individual sources. For the other 93 sources, the exact year of the last event is known by historical reports, while for four of them the date is estimated with a degree of uncertainty of the order of 50% by paleoseismological information. The average elapsed time since the latest event is 228 years with a standard deviation of 262 years. In a couple of cases out of all the 93 sources, the date of the penultimate event can be inferred from historical reports and for other 9 of them, it can be estimated with an error of about 50% by paleoseismological observations. This means that it is impossible to estimate the recurrence time directly from historical series of events, but for some of them paleoseismological series are available.

[42] While the dates of the events in historical catalogs are generally well constrained, it could be questionable if the fault assignments for these events (especially the oldest ones) are certain. Again, we repeat that the aim of this study is not to assess the reliability of the data stored in the DISS database. We assume that this information has been obtained with the highest possible accuracy, and use it for analyzing the consequences on the earthquake hazard through our statistical models.

[43] It is interesting to make a comparison between the time elapsed since the latest event and the recurrence time for each individual source. We have computed the logarithmic average of the minimum and maximum recurrence time for each individual source, whose average is 2020 years with a standard deviation of 1060 years. We have then computed, for each seismogenic source, the ratio between the elapsed time and the minimum, average and maximum recurrence time. The average of these ratios is respectively 0.262, 0.129 and 0.070. Considering the average recurrence time, only for one source the ratio is larger than 1. This means that the elapsed time of the earthquakes related to the individual sources reported in DISS 3.0.2 is much shorter than the respective recurrence time, even considering its shortest values.

[44] In addition to the individual sources, the DISS latest version (3.0.3) stores seismogenic areas, crustal bodies capable of $M \geq 5.5$ earthquakes for which a geographic outline, predominant faulting mechanism, effective depth, and expected maximum magnitude are supplied. A seismogenic area is essentially an inferred structure based on regional surface and subsurface geological data that are exploited well beyond the simple identification of active faults. The effective depth of the seismogenic area is determined by the combined analysis of four data: depth distribution of instrumental earthquakes, geological sections across the active fault system, rheological profiles of the region, seismic tomography and combined analysis with the estimation of width of the region. In many cases, these seismogenic areas have an elongated, slightly curved, shape, and are not associated to a unique characteristic earthquake [*Basili et al.*, 2008].

3.2. The Case of Sources With Paleoseismological Information

[45] As stated above, for some of the individual sources of the DISS database falling in the area of our analysis, results of paleoseismological observations are also available [*Pantosti et al.*, 1993]. The information used in this study has been obtained from the Database of ''Earthquake recurrence from paleoseismological data'' developed in the frame of the ILP project ''Earthquake Recurrence Time'' (http://www.ingv.it/~wwwpaleo/ilp) [*Pantosti*, 2000]. We have considered these data with the aim of obtaining the mean recurrence time T_r and the aperiodicity α for some of the sources. For our study area, Table 1 reports the occurrence times of the characteristic earthquakes obtained by C^{14} dating technique, with their error range, except for the events for which historical reports do exist and there is no uncertainty on the year of occurrence.

[46] We compute the mean recurrence time $\overline{T}_r$ for each time series by averaging the time differences between pairs of consecutive earthquakes. This means that for the series of which only three events have been dated, only two inter-event times are available. Occurrence times are generally reported with a wide range of uncertainty. *Rhoades et al.* [1994] and *Rhoades and Van Dissen* [2003] have analyzed theoretically the problem of reporting uncertainties and their

Table 2. Parameters of the BPT Renewal Model for the Faults for Which Paleoseismological Data are Available

Source Code	Source Name	$\overline{T}_r$ Paleoseismological, yr	T_r Geodetic, yr	$\overline{\alpha}$
ITGG001	Ovindoli-Pezza	5080 ± 2251	2571	0.497 ± 0.287
ITGG002	Fucino Basin	1723 ± 137	3301	0.270 ± 0.104
ITGG003	Aremogna	2239 ± 397	2733	0.626 ± 0.202
ITGG077	Irpinia (Colliano)	2246 ± 167	11531	0.355 ± 0.110
ITGG096	Isola del Gran Sasso	9859 ± 2629	22404	0.445 ± 0.186

implication on hazard assessment in great detail. More recently, *Parsons* [2008] has published a thorough study about earthquake recurrence parameters and their uncertainties from short paleoseismic catalogs applying a Monte Carlo method. His study focuses with particular attention on the cases when the paleoseismic records encompass a small (10 or less) number of events. Our database shown in Table 1 is characterized by a dramatically smaller number of events, ranging from 3 to 6 for all the six considered paleoseismological series. Note that the ITGG077 Irpinia series includes an open interval for the oldest event. In principle this is a piece of information that could contribute to constrain the recurrence time. However, in this exercise, in order to have a homogeneous procedure among all the six paleoseismological series, we have simply ignored such information. The number of known events is therefore only 5 (i.e. 4 inter-event times) also for this specific series.

[47] Here in order to take account of the dating uncertainties in the occurrence time of each paleoseismological event, we apply a Monte Carlo technique, though following a different procedure from that developed by *Parsons* [2008]. Each occurrence time is drawn randomly and with a uniform probability density within the interval of uncertainty of each single event in a series, and the process is repeated one thousand times. Averaging over the one thousand outcomes, we obtain not only the mean recurrence time, which is virtually identical to the arithmetic mean of the inter-event times taken between the central points of each interval of uncertainty, but also its standard deviation for a specific source. For the estimate of the aperiodicity α and its standard deviation we apply a similar procedure: A single value of the aperiodicity is computed by the ratio of the standard deviation and mean recurrence time from a random draw of the occurrence time for each single event within its interval of uncertainty. Again, the average aperiodicity and its standard deviation is computed from the set of one thousand outcomes of the Monte Carlo procedure. The results of these computations are reported in Table 2. We shall discuss in section 4.1 the clear discrepancies between the recurrence times obtained from the paleoseismological information and the geodetic strain, respectively.

[48] Computing the standard deviation on aperiodicity (which is itself a standard deviation divided by the mean) may be a confusing procedure. For sake of clarification, we recall that the mean and the standard deviation for the computation of the aperiodicity relatively to a single series are computed over the few (2–4) inter-event times of such series. The Monte Carlo procedure reiterates the same computations a large (i.e. 1000) number of times with a random choice of the occurrence times within the respective uncertainty intervals of every earthquake. Then the average and the standard deviation of the one thousand results are computed. This overall standard deviation of the aperiodicity can be regarded a way of assessing the confidence intervals associated with the uncertainty of the paleoseismological datings. If all the uncertainty intervals had a zero width (i.e. for a series composed by historical earthquakes only), the standard deviation of the aperiodicity would consequently be zero.

[49] It is obvious that the small number of events reported for each fault, makes the statistical meaning of the results very poor. This is particularly true for the cases of faults with only three events reported. For these three faults the observed aperiodicity is ranging about 0.5, while for the other two (Fucino and Irpinia), it is significantly smaller. Note also that for the latter sources (ITGG002 and ITGG077) the standard deviation for the aperiodicity is smaller than for the others, and only of the order of 0.1. This is clearly related to the narrow intervals of uncertainty of the paleoseismic datings.

[50] Note that two of the faults (Ovindoli-Pezza and Isola del Gran Sasso) exhibit a much larger average recurrence time with respect to the others. This is clearly due to the fact that the oldest event on these faults is dated with a very large uncertainty.

[51] As noted by *Ellsworth et al.* [1999] and discussed in great detail by *Parsons* [2008], both the recurrence time T_r and the aperiodicity α obtained from a sample of a small number of inter-event times are affected by large uncertainties. Generally, the estimate of these parameters for series containing less than 10 events are considered unreliable. It can be also shown that these estimates are systematically biased with respect to the theoretical values of the same parameters that would be obtained from a large number of observations (I. Mosca et al., Renewal models of seismic recurrence applied to paleoseismological data, submitted to *Tectonophysics*, 2008). The reason of this bias can be ascribed to the fact that the records containing events whose intervals are observed have a limited length. So the longest inter-event times are systematically eliminated from the average. For instance, the average inter-event time estimated from records of 1000 years, all containing two events, is 333 years. If there are three events in 1000 years, the average interval between them is 250 years, and so on. In order to assess and correct this effect, we have adopted a bootstrap procedure. This procedure consists in making synthetic sequences, modelled by a BPT (or eventually an exponential) distribution with assigned parameters, with the same number of events and the same total time covered by the observed data. The computer code allows the arbitrary choice of the recurrence time (input) and of the coefficient of variation α (input). For each of these synthetic distributions, the corresponding T_r (output) and α (output) are computed. Repeating the procedure one thousand times, we obtain an average T_r (output) and α (output), which are generally different from the respective input parameters of

Table 3. Theoretical and Apparent Parameters of the Renewal Model for the Faults for Which Paleoseismological Data are Available

Source Code	Source Name	$\overline{T}_r$ (Input), yr	$\overline{\alpha}$ (Input)	$\overline{T}_r$ (Output), yr	$\overline{\alpha}$ (Output)
ITGG001	Ovindoli-Pezza	6667	1.00[a]	5080 ± 2251	0.497 ± 0.289
ITCC002	Fucino Basin	1900	0.350	1682 ± 289	0.256 ± 0.106
ITG0003	Aremogna	2933	1.00[a]	2235 ± 1212	0.497 ± 0.289
ITGG077	Irpinia (Colliano)	3000	0.500	2166 ± 833	0.366 ± 0.135
ITGG096	Isola del Gran Sasso	13000	1.00[a]	9906 ± 4390	0.497 ± 0.289

[a]Poisson model adopted.

the parent distribution, and we call average apparent estimates. By means of a trial and error search, it is easy to find a pair of input parameters T_r (input) and α (input) that provides output values close to those observed from the real seismic sequence. We assume that these input parameters are those of an ideal process that would exhibit the same apparent parameters of the real one in the same observational situation. The results of these simulations, reported in Table 3, confirm that both the apparent recurrence time T_r (output) and the apparent coefficient of variation α (output) are significantly smaller than the respective T_r (input) and α (input) of the parent distributions.

[52] This procedure has a similar aim, though conceptually different from the Monte Carlo procedure developed by *Parsons* [2008]. The latter starts with the same random draw of a series of events under a BPT distribution of randomly chosen parameters. Then, the set of parameters is tallied if the events of the synthetic series fall all within the interval of uncertainty of the real observed earthquake series. The process is reiterated until a consistent number of synthetic series matching the real one is obtained. This method requires millions of iterations for matching series composed by a fairly large number of events (let say larger than 10), and narrow intervals of uncertainty.

[53] In spite of the substantial difference between the approach adopted in this study and that described by *Parsons* [2008], it is clear that both procedures consistently show a systematic underestimation of the parameters obtained directly from the observed inter-event times, when series containing very few events are analyzed. A clear example is given by *Parsons* [2005, Figures 3 and 4].

[54] For the three sources that have only three events (i.e., two inter-event times) reported, we decided to adopt a plain Poisson model for the recurrence time distribution given as input of the simulations. This is justified by the fact that for a sequence composed by three events only, even if it is

Table 4. Source Parameters of the Faults Considered in This Study

Source Code	Source Name	Latest Event	M	Depth, km	Length, km	Width, km	Slip, m	Strike	Dip	Rake
ITGG001	Ovindoli-Pezza	860	6.6	7.5	27.0	15.0	0.80	150 ± 20	57.5 ± 7.5	270 ± 10
ITGG002	Fucino Basin	13 January 1915	6.7	7.6	28.0	15.4	1.06	150 ± 20	57.5 ± 7.5	270 ± 10
ITGG003	Aremogna-Cinque Miglia	800 B.C.	6.4	6.3	20.0	12.2	0.66	145 ± 10	60 ± 5	270 ± 10
ITGG004	Boiano Basin	26 July 1805	6.6	6.6	24.0	13.8	0.97	315 ± 15	55 ± 5	270 ± 10
ITGG005	Tammaro Basin	6 May 1688	6.6	7.2	25.0	14.3	0.90	315 ± 15	55 ± 5	270 ± 10
ITGG006	Ufita Valley	29 November 1732	6.6	7.3	26.0	14.7	0.84	280 ± 10	65 ± 10	240 ± 10
ITGG008	Agri Valley	16 December 1857	6.5	6.8	23.0	13.5	0.74	315 ± 15	60 ± 10	270 ± 10
ITGG010	Melandro-Pergola	16 December 1857	6.5	5.9	17.9	11.3	0.57	310 ± 10	60 ± 10	270 ± 10
ITGG015	Montereale Basin	2 February 1703	6.5	6.9	23.4	13.6	0.72	150 ± 20	57.5 ± 7.5	270 ± 10
ITGG016	Norcia Basin	14 January 1703	6.5	7.2	25.0	14.3	0.64	150 ± 20	57.5 ± 7.5	270 ± 10
ITGG019	Sellano	14 October 1997	5.6	4.5	6.0	6.0	0.28	142.5 ± 7.5	40 ± 5	270 ± 10
ITGG020	Monte Sant'Angelo	1273	6.4	5.9	20.0	12.0	0.67	275 ± 15	85 ± 5	215 ± 15
ITGG022	San Marco Lamis	6 December 1875	6.1	5.9	10.0	12.0	0.48	275 ± 15	85 ± 5	215 ± 15
ITGG026	Amatrice	7 October 1639	6.1	5.3	14.0	9.5	0.43	145 ± 15	60 ± 5	270 ± 10
ITGG027	Sulmona Basin	3 December 1315	6.4	6.3	20.0	12.2	0.66	145 ± 15	60 ± 5	270 ± 10
ITGG028	Barrea	7 May 1984	5.8	7.8	10.0	7.5	0.27	150 ± 20	57.5 ± 7.5	270 ± 10
ITGG052	San Giuliano di Puglia	31 October 2002	5.8	15.9	10.5	8.0	0.20	260 ± 10	85 ± 5	200 ± 20
ITGG053	Ripabottoni	1 November 2002	5.7	16.0	9.4	8.0	0.18	260 ± 10	85 ± 5	200 ± 20
ITGG054	San Severo	30 July 1627	6.8	13.4	34.0	15.0	0.90	260 ± 10	85 ± 5	200 ± 20
ITGG061	Foligno	13 January 1832	5.8	3.5	10.2	6.0	0.35	305 ± 25	32.5 ± 7.5	270 ± 10
ITGG062	Trevi	15 September 1878	5.5	3.1	7.0	4.5	0.25	305 ± 25	32.5 ± 7.5	270 ± 10
ITGG070	Offida	3 October 1943	5.9	6.6	7.9	7.4	0.40	160 ± 10	40 ± 10	90 ± 10
ITGG077	Colliano	23 November 1980	6.8	7.5	28.0	15.0	1.65	310 ± 10	60 ± 10	270 ± 10
ITGG078	San Gregorio Magno	23 November 1980	6.2	7.5	9.0	15.0	0.70	310 ± 10	60 ± 10	270 ± 10
ITGG079	Pescopagano	23 November 1980	6.2	5.7	15.0	10.0	0.50	125 ± 10	70 ± 10	270 ± 10
ITGG080	Cerignola	20 March 1731	6.3	16.5	18.6	11.3	0.60	270 ± 10	80 ± 10	180 ± 10
ITGG081	Melfi	14 August 1851	6.3	17.4	17.2	11.0	0.66	270 ± 10	80 ± 10	180 ± 10
ITGG082	Ascoli Satriano	17 July 1361	6.0	17.1	12.6	8.4	0.42	270 ± 10	80 ± 10	180 ± 10
ITGG083	Bisceglie	11 May 1560	5.7	16.1	8.6	6.3	0.29	270 ± 10	80 ± 10	180 ± 10
ITGG084	Potenza	5 May 1990	5.7	17.9	7.9	6.2	0.26	90 ± 10	85 ± 5	180 ± 10
ITGG088	Bisaccia	23 July 1930	6.7	10.2	29.4	16.0	0.95	280 ± 10	65 ± 10	240 ± 10
ITGG092	Ariano Irpino	5 December 1456	6.9	18.0	30.0	14.9	2.00	280 ± 10	70 ± 10	230 ± 10
ITGG094	Tocco da Casauria	30 December 1456	6.0	14.7	12.0	8.0	0.45	90 ± 10	80 ± 10	200 ± 30
ITGG095	Frosolone	30 December 1457	7.0	18.0	36.0	14.9	2.50	270 ± 10	70 ± 10	230 ± 10
ITGG096	Isola del Gran Sasso	5 September 1950	5.7	14.9	10.0	6.0	0.25	90 ± 10	80 ± 10	200 ± 30

modelled by a plain Poisson distribution, the apparent aperiodicity obtained by the Monte Carlo procedure described above, from a time-independent random choice of occurrence times, is very close to 0.5. There is no point in adopting a two-parameter model if a single parameter model does the same job.

[55] The main results of this analysis are:

[56] For only two faults (Fucino Basin and Irpinia) the paleoseismological data provide evidence of a quasiperiodical behavior of the occurrence times for the characteristic earthquakes;

[57] For these two faults the statistical analysis allows to correct a biasing effect due to the limited number of events in the sample, that significantly reduces the apparent average value of the recurrence time and coefficient of variation obtained from the observations;

[58] Taking into account this biasing effect, only for the Fucino Basin fault the adoption of a coefficient of variation smaller than 0.5 seems justified;

[59] For two of the other three faults the time limits by which the oldest event is dated are too large to give a meaningful assessment of the average inter-event time;

[60] For the remaining fault (Aremogna), the paleoseismological observations provide a fairly reliable estimate of the average recurrence time; however, a set of only two inter-event times does not allow a reliable estimate of the coefficient of variation α;

[61] The results of statistical simulations show that a value of 0.5 for the aperiodicity is likely to be obtained as an artifact caused by the limited number of events for which the occurrence time is known, in this case only three, even if the parent distribution is obtained from a Poissonian model.

4. Data Analysis

[62] We apply the methodology outlined in section 2 to a selected set of the earthquake sources shown in Table 4 whose characteristics are described in section 3. The purpose of this exercise is comparing the hazard estimated by a simple Poisson model with that deduced from a renewal time-dependent model, without and with the consideration of both the permanent and transient effect of the Coulomb stress change. In this way, we shall also assess the impact of uncertainties affecting the relevant parameters used in the models on the results.

4.1. The Selected Sources and Their Poissonian and Renewal Recurrence Models

[63] Table 4 shows, for the 35 individual sources included in the rectangle of coordinates 40°–43°N and 13°–17°E (Figure 1), the code, name, date of the latest earthquake (unknown for three of them), the expected magnitude, depth, size, slip and focal mechanism, as reported by the DISS 3.0.2 database. It is remarkable that in one case two different sources (ITGG008 and ITGG010) nucleated their latest characteristic earthquake nearly at the same time (producing one event known as the Val D'Agri earthquake of 16 December 1857). Another, even more complicated case reported in DISS 3.0.2 consists in the almost simultaneous rupture of three different sources (ITGG077, ITGG078 and ITGG079, the latter of which characterized by a significantly different focal mechanism with respect to the others) in the most recent 23 November 1980, destructive Irpinia earthquake, These two cases may well represent the phenomenon of instantaneous triggering described by *Zöller and Hainzl* [2007]. We can infer that multiple ruptures could have happened also in other strong earthquakes, reported by historical catalogs as only one event because of the poor time resolution. As it seems unjustified to assume that the above mentioned Val D'Agri and Irpinia sources have ruptured simultaneously in the past events, and will rupture simultaneously in future, in this study we have considered them as separate sources. However, we have neglected the effect of stress interaction of the two and three segments of these multiple ruptures among themselves.

[64] The study area is dominated by a fairly uniform extensional regime with a sub-horizontal σ_3 axis normal to the Apenninic trend (i.e. South/West–North/East direction). Most of the sources exhibit a normal focal mechanism characterized by North/West–South/East strike, but we can also observe right-lateral strike-slip faults with almost pure east–west trend.

[65] Although no evidence, except for the ITGG003 (Fucino Basin) and ITGG077 (Irpinia) faults, exists of a renewal behavior of the inter-event times on the Italian individual sources, in this study we apply the BPT renewal model with the purpose of a methodological investigation about its properties. In order to make use of the BPT model described by equation (5), we need the mean recurrence time T_r, the aperiodicity parameter α, and the time elapsed since the latest event for each of the 35 seismogenic sources. These parameters are known with a different degree of accuracy and reliability.

[66] The recurrence time is, together with the slip rate, the parameter reported with the largest degree of uncertainty in DISS 3.0.2. As recalled above, these two parameters are linked together for a single characteristic earthquake. For sake of comparison, besides the recurrence times from DISS 3.0.2 with their large error range, we make use, whenever possible, of the most recent information available from the literature about the strain rate obtained through geodetic (GPS) measurements in the Italian region [*Serpelloni et al.*, 2005]. The slip rate can be obtained from the strain rate (resolved on the slip direction of every specific fault) through a method described in Appendix A. The strain rate and the slip rate are reported, with their uncertainties, respectively in column 3 and 4 of Table 5. The average slip (reported by DISS 3.0.2 with high accuracy for each individual source), divided by the slip rate, gives the average inter-event time of the characteristic event. An alternative method for obtaining the recurrence time could be estimating the tectonic stress rate on every source through the strain rate obtained by geodetic observations. Assuming that the stress drop is fairly constant for every characteristic earthquake, the average inter-event time of this characteristic earthquake should be equal to the average value of the stress drop divided by the tectonic stress rate. We show in Appendix A that these two procedures are not independent of each other, both being based on the hypothesis of a constant known stress drop. Another important assumption on which both procedures are based is that all the tectonic strain is released through characteristic earthquakes. However, according to the Guntenberg-Richter

Table 5. Characteristic Parameters of the Seismogenic Sources Considered in This Study

Source Code	Source Name	Strain Rate, 10^{-9}/yr	Slip Rate, mm/yr	Recurrence Time, yr	Coefficient of Variation Adopted
ITGG001	Ovindoli-Pezza	31 ± 8	0.31 ± 0.08	3984 ± 2684	0.7 ± 0.3
ITGG002	Fucino Basin	31 ± 8	0.32 ± 0.08	19002925 ± 330	0.35 ± 0.10
ITGG003	Aremogna-Cinque Miglia	31 ± 8	0.24 ± 0.06	3610 ± 1470	0.7 ± 0.3
ITGG004	Boiano Basin	14 ± 5	0.14 ± 0.05	5958 ± 4988	0.7 ± 0.3
ITGG005	Tammaro Basin	14 ± 5	0.11 ± 0.07	11055 ± 10155	0.7 ± 0.3
ITGG006	Ufita Valley	14 ± 5	0.11 ± 0.07	9949 ± 9109	0.7 ± 0.3
ITGG008	Agri Valley	15 ± 5	0.13 ± 0.04	4580 ± 3840	0.7 ± 0.3
ITGG010	Melandro-Pergola	15 ± 5	0.11 ± 0.04	4303 ± 3733	0.7 ± 0.3
ITGG015	Montereale Basin	31 ± 8	0.28 ± 0.07	3960 ± 3240	0.7 ± 0.3
ITGG016	Norcia Basin	31 ± 8	0.29 ± 0.08	5870 ± 4130	0.7 ± 0.3
ITGG019	Sellano	31 ± 8	0.11 ± 0.03	2140 ± 1440	0.7 ± 0.3
ITGG020	Monte Sant'Angelo	20 ± 0	0.09 ± 0.00	4106 ± 3406	0.7 ± 0.3
ITGG022	San Marco Lamis	20 ± 0	0.06 ± 0.00	4155 ± 3455	0.7 ± 0.3
ITGG026	Amatrice	31 ± 8	0.16 ± 0.04	2375 ± 1300	0.7 ± 0.3
ITGG027	Sulmona Basin	31 ± 8	0.24 ± 0.06	2313 ± 1371	0.7 ± 0.3
ITGG028	Barrea	31 ± 8	0.15 ± 0.04	1700 ± 1000	0.7 ± 0.3
ITGG052	San Giuliano di Puglia	20 ± 0	0.05 ± 0.00	2245 ± 1545	0.7 ± 0.3
ITGG053	Ripabottoni	20 ± 0	0.05 ± 0.00	2153 ± 1453	0.7 ± 0.3
ITGG054	San Severo	20 ± 0	0.13 ± 0.00	4950 ± 4050	0.7 ± 0.3
ITGG061	Foligno	5 ± 8	0.12 ± 0.03	2301 ± 1601	0.7 ± 0.3
ITGG062	Trevi	31 ± 8	0.09 ± 0.02	2292 ± 1592	0.7 ± 0.3
ITGG070	Offida	31 ± 8	0.03 ± 0.02	16468 ± 15768	0.7 ± 0.3
ITGG077	Colliano	5 ± 5	0.14 ± 0.05	3000 ± 1150	0.50 ± 0.15
ITGG078	San Gregorio Magno	5 ± 5	0.08 ± 0.03	7551 ± 5871	0.7 ± 0.3
ITGG079	Pescopagano	14 ± 5	0.06 ± 0.02	6965 ± 5285	0.7 ± 0.3
ITGG080	Cerignola	14 ± 0	0.08 ± 0.00	3944 ± 3244	0.7 ± 0.3
ITGG081	Melfi	14 ± 5	0.06 ± 0.02	9610 ± 8910	0.7 ± 0.3
ITGG082	Ascoli Satriano	20 ± 3	0.05 ± 0.01	5415 ± 4715	0.7 ± 0.3
ITGG083	Bisceglie	14 ± 3	0.02 ± 0.01	8904 ± 8204	0.7 ± 0.3
ITGG084	Potenza	17 ± 5	0.03 ± 0.01	7520 ± 6820	0.7 ± 0.3
ITGG088	Bisaccia	11 ± 5	0.09 ± 0.03	8928 ± 7978	0.7 ± 0.3
ITGG092	Ariano Irpino	14 ± 5	0.09 ± 0.03	19256 ± 17256	0.7 ± 0.3
ITGG094	Tocco da Casauria	14 ± 8	0.07 ± 0.03	6552 ± 5852	0.7 ± 0.3
ITGG095	Frosolone	14 ± 0	0.13 ± 0.00	13750 ± 11250	0.7 ± 0.3
ITGG096	Isola del Gran Sasso	18 ± 8	0.04 ± 0.02	6850 ± 6150	0.7 ± 0.3

frequency-magnitude law, a part of the seismic moment is also released by smaller earthquakes. The problem has been analyzed in detail by *Field et al.* [1999], but we have followed the approximation of ignoring the contribution of smaller earthquakes, in consideration of the large uncertainties that affect other parts of the procedures.

[67] Columns 3 and 4 of Table 2 allow a comparison between the (uncorrected) paleoseismological and geodetic recurrence times computed for the same five faults. The results appear quite inconsistent, and without a systematic trend. The largest discrepancy concerns the Irpinia fault, for which the geodetic value is larger than the paleoseismological one by a factor of five times. This circumstance can be ascribed to the low strain rate reported by *Serpelloni et al.* [2005] for the whole region, and explained by the fact that the geodetic strain is the average over a wide region, some areas of which could exhibit strain concentrations.

[68] It appears clearly that the geodetic estimates of the recurrence times are characterized by much narrower uncertainties than the DISS 3.0.2 estimates. Nevertheless, we consider the geodetic estimates not so reliable as they appear from the observation errors only, because of possible systematic unknown factors, such as the fraction of strain released aseismically (or from the smaller earthquakes) and the inaccuracy due to the very sparse grid of geodetic stations that could encompass areas of inhomogeneous strain rate.

[69] To keep track the large uncertainties and discrepancies that affect the recurrence times of most of the 35 sources considered in our study, we have adopted the most conservative approach. We have taken the minimum and maximum among the values obtained from DISS 3.0.2 or from the geodetic method, with their uncertainties, and computed their mean. We have also included the paleoseismic values in the same computation, when they were available. Only for the Fucino (ITGG002) and Colliano (ITGG077) faults we have retained the paleoseismological information most reliable and adopted the paleoseismological recurrence times with their associated uncertainties. For the error analysis reported later in section 5, we shall take in consideration the largest uncertainty interval spanned by the various methods. The central values of the recurrence times and their uncertainties are reported in column 5 of Table 5.

[70] As for the recurrence times, for the 35 individual sources of this study the coefficients of variation (or aperiodicity) α, cannot be inferred from historical sequences of events on the same fault. In fact, this information is unknown, due to the fact that the recurrence time is generally longer than the duration of the historical record. In consideration of the methodological character of our work, we decided to consider a wide range of values, starting from $\alpha = 0.4$ (adopted by *Wells and Coppersmith* [1994]) up to the upper limit of $\alpha = 1.0$. We recall that *Ellsworth et al.* [1999] and *Matthews et al.* [2002] adopted for this parameter the value $\alpha = 0.5$. Only for the Fucino fault, the paleoseismological data (see the detailed analysis in section 3.2 above) suggest the adoption of a smaller

Table 6. Poissonian and Conditional Probability of Occurrence of the Seismogenic Sources for the Next 50 Years After 1 January 2007

Source Code	Source Name	$P_{Poisson}(50)$	Elapsed Time, yr	$P_{cond}(50)$
ITGG001	Ovindoli-Pezza	1.90e − 02	1147	1.48e − 02
ITGG002	Fucino Basin	2.60e − 02	92	0.00e + 00
ITGG003	Aremogna-Cinque Miglia	1.69e − 02	2807	3.24e − 02
ITGG004	Boiano Basin	7.08e − 03	202	0.00e + 00
ITGG005	Tammaro Basin	7.31e − 03	319	0.00e + 00
ITGG006	Ufita Valley	8.09e − 03	275	0.00e + 00
ITGG008	Agri Valley	8.87e − 03	150	0.00e + 00
ITGG010	Melandro-Pergola	9.29e − 03	150	0.00e + 00
ITGG015	Montereale Basin	1.90e − 02	304	2.16e − 06
ITGG016	Norcia Basin	2.26e − 02	304	2.32e − 05
ITGG019	Sellano	2.35e − 02	10	0.00e + 00
ITGG020	Monte Sant'Angelo	3.66e − 02	734	4.24e − 02
ITGG022	San Marco Lamis	1.04e − 02	132	0.00e + 00
ITGG026	Amatrice	2.53e − 02	368	4.09e − 04
ITGG027	Sulmona Basin	4.44e − 02	692	6.20e − 02
ITGG028	Barrea	1.89e − 02	23	0.00e + 00
ITGG052	San Giuliano di Puglia	2.47e − 02	5	0.00e + 00
ITGG053	Ripabottoni	2.74e − 02	5	0.00e + 00
ITGG054	San Severo	7.20e − 03	380	0.00e + 00
ITGG059	Velletri	1.65e − 02	201	0.00e + 00
ITGG061	Foligno	1.71e − 02	175	0.00e + 00
ITGG062	Trevi	1.72e − 02	129	0.00e + 00
ITGG068	Casamicciola	1.65e − 02	124	0.00e + 00
ITGG070	Offida	1.24e − 02	64	0.00e + 00
ITGG077	Colliano	1.65e − 02	27	0.00e + 00
ITGG078	San Gregorio Magno	1.58e − 02	27	0.00e + 00
ITGG079	Pescopagano	1.58e − 02	27	0.00e + 00
ITGG080	Cerignola	8.30e − 03	276	0.00e + 00
ITGG081	Melfi	7.55e − 03	156	0.00e + 00
ITGG082	Ascoli Satriano	1.18e − 02	646	2.20e − 05
ITGG083	Bisceglie	1.71e − 02	447	3.96e − 05
ITGG084	Potenza	1.90e − 02	17	0.00e + 00
ITGG088	Bisaccia	5.25e − 03	77	0.00e + 00
ITGG092	Ariano Irpino	2.50e − 03	551	0.00e + 00
ITGG094	Tocco da Casauria	1.10e − 02	551	1.41e − 06
ITGG095	Frosolone	2.66e − 03	551	0.00e + 00
ITGG096	Isola del Gran Sasso	2.00e − 02	57	0.00e + 00

coefficient of variation, that is $\alpha = 0.35 \pm 0.1$, as reported in column 6 of Table 5.

[71] For purposes of comparison, our analysis includes also the hypothesis that the events behave as a plain Poisson time-independent model, for which $\alpha = 1.0$. The time-independent probabilities of occurrence for the next 50 years, under this hypothesis, are reported in column 3 of Table 6.

[72] Finally, we must take into consideration the time elapsed since the latest event on every fault. This piece of information is reported in DISS 3.0.2 for all the sources of the study area, except for three individual sources (ITGG001, ITGG003 and ITGG020), for which no reliable historical report is available. For the first two of these faults (Ovindoli-Pezza and Aremogna), we make use of paleoseismological information, adopting the mean of the occurrence time range as elapsed time. For ITGG020 (Monte Sant'Angelo) the half of the recurrence time reported in Table 5 is taken as the most probable elapsed time. The elapsed times, estimated in this way for all the 35 sources are reported in column 4 of Table 6.

[73] As shown in section 2, the computation of the hazard function conditional to the time elapsed since the latest characteristic earthquake, under the BPT renewal model, allows the estimate of the probability of occurrence of the next possible event in a future time interval (in our case assumed 50 years long starting on January 2007). Having considered the mean values for all the parameters, we obtained the probabilities reported in the last column of Table 6 for each of the seismogenic sources.

4.2. The Permanent Effect of Stress Changes

[74] We must now consider how the stress changes caused by earthquakes occurred on neighboring faults might affect the probability of occurrence of future earthquakes on the individual sources.

[75] Among the causative events that could have potentially changed the stress conditions on the 35 studied faults, we have considered:

[76] 1. The characteristic events associated to the seismogenic sources themselves (as reported in DISS 3.0.2);

[77] 2. The events reported in the Parametric Catalog of the historical Italian earthquakes [*CPTI04*, 2004] associated to the DISS 3.0.3 seismogenic areas (120 events with $M_w \geq 5.0$).

[78] 3. The events reported in the *CSI* [2007] catalog for the years 1986–2002, updated by those reported in the more recent INGV bulletins (2003–2006), ($M_l \geq 5.0$).

[79] Obviously, all these events have been considered only once in case that they were reported by more than one information source, with preference to the information coming from the source in the order as they are listed.

[80] The stress change ΔCFF on an individual fault is computed adding the contributions from all the other sources that have ruptured after the latest known earthquake on the considered fault. The computation is carried out at

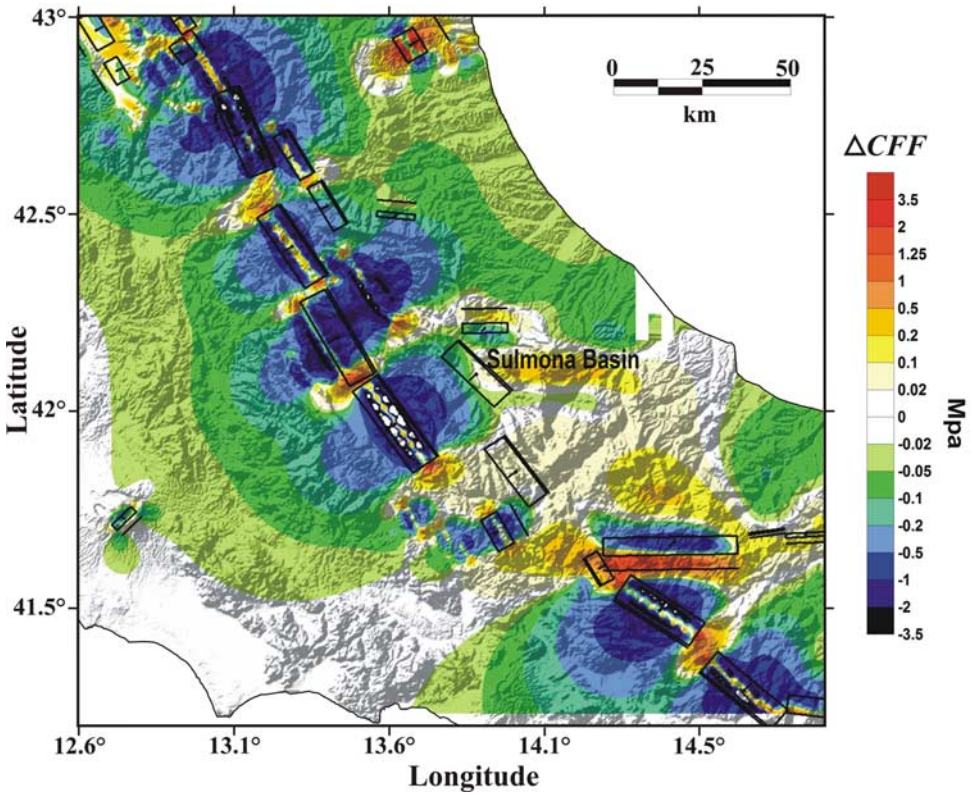

Figure 2. Coulomb failure function change (ΔCFF) at a depth of 6.8 km caused by all the relevant earthquakes occurred after 3 December 1315. The induced focal mechanism adopted for resolving the Coulomb Failure Function (ΔCFF) is the same as that of the Sulmona Basin earthquake.

the hypocentral depth of this latest earthquake, as reported in Table 4. Of course, this is just an assumption because we ignore the depth of the real nucleation point of every source, where the next characteristic earthquake will be initiated. However, a small change in the depth where ΔCFF is estimated doesn't critically affect the results.

[81] Every single contribution is computed by equation (6) through the method explained in section 2. The effective coefficient of friction adopted in this study is $\mu' = 0.5 \pm 0.2$. As the stress change is spatially variable, and the horizontal projection of every individual source is a rectangle with a given size, there is not a univocal solution for the value of ΔCFF to be used in equation (9). So we have considered three different choices for this parameter: the minimum, mean, and maximum computed values and consequently we have also obtained three different clock changes values (Table 7). As an example, the computation of ΔCFF on the Sulmona Basin individual source is shown in Figure 2. It is possible to note how the subsequent events caused on the different parts of this structure a stress change ranging from -0.1 and $+0.06$ MPa. The positive change leads to an advance of the expected occurrence time (clock change) of the next earthquake on the concerned source.

[82] For the computation of the clock change through equation (7), we need the knowledge of the tectonic stressing rate $\dot{\tau}$. To do so, as for the estimation of the recurrence times, the strain tensor has been resolved on the specific source taking into account the mechanism of its characteristic earthquakes. The time change is positive (the fault becomes closer to failure) if the Coulomb stress change is positive. In the opposite case (negative change) the fault becomes farther from failure.

[83] Table 7 contains, for our 35 seismogenic sources, the physical parameters relevant for the computation of the clock advance: the stress rate obtained from geodetic observations, the stress change caused by the subsequent earthquakes, and the time change. For each of the latter two parameters, the minimum, mean and maximum values are reported.

[84] By the use of equation (7), that affects the elapsed time, rather than the equivalent recurrence time, we computed the minimum, mean and maximum probabilities of occurrence of the next characteristic event on the studied seismogenic sources, under the effect of the stress changes (Table 8). These values, which have been computed starting from the mean values for the parameters of the BPT model, should be compared with the corresponding values of the Poissonian and conditional probabilities shown in Table 6.

4.3. The Transient Effect of Stress Changes

[85] As described in the method section, a stress change caused by an earthquake occurred on a neighboring fault, may produce a temporary effect of increasing or reducing the hazard rate for the next earthquake on the considered fault. This change is then followed by a decay toward the previous steady state, as described by equation (9), modeled by the rate-and-state friction law [*Dieterich*, 1994].

[86] The application of the rate-and-state theory to our 35 seismogenic sources has been carried out by means of an algorithm implemented on a computer code. This algorithm

Table 7. Physical Parameters Used for Computing the Time Change

Source Code	Source Name	Stress Rate, (Pa/yr)	Minimum ΔCFF, (MPa)	Mean ΔCFF, (MPa)	Maximum ΔCFF, MPa	Minimum Δt, (years)	Mean Δt, (years)	Maximum Δt, (years)
ITGG001	Ovindoli-Pezza	1503.8 ± 388.1	−7.08	−2.03	1.51	−6349.03	−1448.32	1351.50
ITGG002	Fucino Basin	1503.8 ± 388.1	−0.95	−0.12	0.63	−851.87	−87.09	565.44
ITGG003	Aremogna-Cinque Miglia	1503.8 ± 388.1	−0.09	0.02	0.13	−83.27	13.58	120.59
ITGG004	Boiano Basin	736.8 ± 263.2	0.00	0.00	0.01	−10.37	6.18	28.77
ITGG005	Tammaro Basin	570.0 ± 351.7	0.04	0.15	0.29	48.49	424.49	1311.30
ITGG006	Ufita Valley	570.5 ± 351.2	−4.11	−1.11	1.24	−18750.49	−3140.83	5648.44
ITGG008	Agri Valley	727.6 ± 242.5	0.00	0.01	0.01	3.40	13.50	30.70
ITGG010	Melandro-Pergola	727.6 ± 242.5	−0.06	0.07	0.19	−117.25	103.31	393.60
ITGG015	Montereale Basin	1503.8 ± 388.1	−1.35	−0.36	0.60	−1209.13	−253.48	539.01
ITGG016	Norcia Basin	1503.8 ± 388.1	−3.29	−0.93	1.03	−2951.49	−663.32	921.78
ITGG019	Sellano	1709.5 ± 441.3	0.00	0.00	0.00	−0.01	0.18	0.49
ITGG020	Monte Sant'Angelo	560.0 ± 0.0	−0.13	0.00	0.11	−228.07	5.12	188.50
ITGG022	San Marco Lamis	560.0 ± 0.0	−0.04	−0.01	0.03	−78.47	−12.09	45.48
ITGG026	Amatrice	1330.3 ± 343.3	−2.50	−0.82	0.31	−2532.08	−656.92	310.78
ITGG027	Sulmona Basin	1503.8 ± 388.1	−0.29	−0.07	0.15	−261.68	−52.62	132.19
ITGG028	Barrea	1709.7 ± 441.2	0.00	0.00	0.00	0.06	0.21	0.45
ITGG052	San Giuliano di Puglia	560.0 ± 0.0	0.00	0.00	0.00	0.03	0.05	0.07
ITGG053	Ripabottoni	560.0 ± 0.0	0.00	0.00	0.00	0.03	0.05	0.07
ITGG054	San Severo	560.0 ± 0.0	−0.20	−0.01	0.22	−350.35	−20.46	389.71
ITGG061	Foligno	1503.3 ± 387.9	−0.04	0.00	0.03	−35.48	−2.34	24.87
ITGG062	Trevi	1503.3 ± 387.9	−0.03	−0.02	−0.01	−30.30	−11.27	−3.41
ITGG070	Offida	421.0 ± 263.1	0.00	0.00	0.01	0.97	11.41	32.07
ITGG077	Colliano	679.1 ± 242.5	0.00	0.00	0.00	0.15	1.62	6.62
ITGG078	San Gregorio Magno	679.1 ± 242.5	0.00	0.00	0.00	−3.54	2.88	10.28
ITGG079	Pescopagano	504.2 ± 180.1	0.00	0.00	0.00	−1.31	0.57	5.06
ITGG080	Cerignola	560.0 ± 0.0	−0.17	−0.10	−0.05	−304.45	−177.25	−94.46
ITGG081	Melfi	392.0 ± 140.0	−0.40	−0.14	0.35	−1584.44	−401.25	1371.26
ITGG082	Ascoli Satriano	476.0 ± 84.0	−0.17	−0.06	0.03	−437.50	−138.33	83.49
ITGG083	Risceglie	308.0 ± 84.0	−0.02	0.01	0.07	−80.09	46.04	318.00
ITGG084	Potenza	392.0 ± 140.0	−0.33	−0.10	0.01	−1322.21	−283.02	43.86
ITGG088	Bisaccia	392.0 ± 140.0	−1.30	−0.31	0.42	−5145.23	−908.85	1649.62
ITGG092	Ariano Irpino	392.0 ± 140.0	−0.39	0.12	0.63	−1544.36	341.18	2514.81
ITGG094	Tocco da Casauria	648.3 ± 288.1	−0.14	0.01	0.18	−395.04	15.02	505.53
ITGG095	Frosolone	560.0 ± 0.0	0.46	0.10	0.46	−371.36	175.60	828.42
ITGG096	Isola del Gran Sasso	504.4 ± 224.2	0.00	0.00	0.00	−2.90	0.69	6.16

computes the hazard rate consequent to the cumulative effect of the earthquakes occurred after the latest event on the individual source under consideration (F. Catalli et al., Modeling seismicity rate changes during the 1997 Umbria-Marche sequence, in central Italy through a rate-and state-dependent model, submitted to *Journal of Geophysical Research*, 2008).

[87] The $A\sigma$ free parameter of the model has been taken from a previous unpublished analysis of the Italian seismicity, that had given the result of $A\sigma = 0.002$ MPa. The hazard rate is computed at a specified date, taking into account the time elapsed after each of the causative earthquakes. The effect is negligible if the causative events occur far in geographical distance and back in time with respect to the considered individual fault.

[88] Table 9 shows, for each of the 35 considered faults, the mean hazard rates as of 1 January 2007 under the four different hypotheses: (1) plain time-independent Poisson model, (2) BPT renewal model conditional to the time elapsed since the latest earthquake, (3) the same BPT model taking into account the permanent effect of stress interaction, and (4) model (5) taking into account the transient effect of stress interaction.

5. Results and Discussion

[89] We examine in the following sub-sections some of the most relevant results obtained from this exercise and make a quantitative analysis of the uncertainties affecting the whole methodology.

5.1. Probability Assessment Under Different Hypotheses

[90] The first remarkable result of our analysis is that for most of the sources, the renewal model forecasts a negligible probability of occurrence for the next 50 years, while for the Poisson model this probability is more uniformly distributed in the range from slightly less than one to a few percent. This is due to the relatively short elapsed time, compared with the mean recurrence time of the seismogenic sources reported by DISS 3.0.2. As a consequence, only for four sources out of the 35 considered in this study the occurrence conditional probability for the next 50 years is larger than one percent (Table 6). Only for three of these four sources (Aremogna-Cinque Miglia, Monte Sant'Angelo and Sulmona) the conditional probability of occurrence obtained from the renewal model is larger than the Poisson one. These are in fact the faults for which the time elapsed since the latest earthquake is not much lower than the recurrence time (column 4 of Table 6 and column 5 of Table 5, respectively).

[91] The evident feature that for the next 50 years the time-dependent renewal model based on the (mean) BPT distribution forecasts a number of events much smaller than the average of the past 300 years appears suspicious for the

Table 8. Probability of Occurrence Modified by the Permanent Effect of ΔCFF on the Seismogenic Faults for the Next 50 Years After 1 January 2007

Source Code	Source Name	Minimum $P_{mod}(50)$	Mean $P_{mod}(50)$	Maximum $P_{mod}(50)$
ITGG001	Ovindoli-Pezza	0.00e + 00	1.86e − 02	1.15e − 01
ITGG002	Fucino Basin	0.00e + 00	6.80e − 05	4.30e − 04
ITGG003	Aremogna-Cinque Miglia	0.00e + 00	2.19e − 02	6.48e − 02
ITGG004	Boiano Basin	0.00e + 00	1.40e − 02	6.02e − 02
ITGG005	Tammaro Basin	0.00e + 00	3.62e − 02	1.60e − 01
ITGG006	Ufita Valley	0.00e + 00	3.04e − 02	1.73e − 01
ITGG008	Agri Valley	0.00e + 00	1.89e − 02	8.02e − 02
ITGG010	Melandro-Pergola	0.00e + 00	4.02e − 02	1.86e − 01
ITGG015	Montereale Basin	0.00e + 00	4.00e − 02	2.01e − 01
ITGG016	Norcia Basin	0.00e + 00	2.00e − 02	1.12e − 01
ITGG019	Sellano	0.00e + 00	4.19e − 04	1.75e − 03
ITGG020	Monte Sant'Angelo	0.00e + 00	5.93e − 02	1.85e − 01
ITGG022	San Marco Lamis	0.00e + 00	1.58e − 02	8.95e − 02
ITGG026	Amatrice	0.00e + 00	1.62e − 02	1.45e − 01
ITGG027	Sulmona Basin	0.00e + 00	3.53e − 02	1.18e − 01
ITGG028	Barrea	0.00e + 00	1.27e − 03	5.25e − 03
ITGG052	San Giuliano di Puglia	0.00e + 00	2.36e − 04	9.54e − 04
ITGG053	Ripabottoni	0.00e + 00	2.36e − 04	9.54e − 04
ITGG054	San Severo	0.00e + 00	2.37e − 02	1.09e − 01
ITGG061	Foligno	0.00e + 00	2.33e − 02	8.97e − 02
ITGG062	Trevi	0.00e + 00	1.66e − 02	7.95e − 02
ITGG070	Offida	0.00e + 00	1.73e − 02	7.00e − 02
ITGG077	Colliano	0.00e + 00	0.00e + 00	0.00e + 00
ITGG078	San Gregorio Magno	0.00e + 00	3.20e − 06	3.05e − 05
ITGG079	Pescopagano	0.00e + 00	2.16e − 06	1.61e − 05
ITGG080	Cerignola	0.00e + 00	1.38e − 02	1.28e − 01
ITGG081	Melfi	0.00e + 00	1.45e − 02	2.08e − 01
ITGG082	Ascoli Satriano	0.00e + 00	4.90e − 02	1.94e − 01
ITGG083	Bisceglie	0.00e + 00	4.77e − 02	1.68e − 01
ITGG084	Potenza	0.00e + 00	3.89e − 02	1.68e − 01
ITGG088	Bisaccia	0.00e + 00	4.20e − 02	1.52e − 01
ITGG092	Ariano Irpino	0.00e + 00	2.29e − 02	9.43e − 02
ITGG094	Tocco da Casauria	0.00e + 00	5.06e − 02	1.92e − 01
ITGG095	Frosolone	0.00e + 00	6.00e − 03	2.74e − 02
ITGG096	Isola del Gran Sasso	0.00e + 00	6.47e − 03	3.06e − 02

credibility of the parameters adopted for this model or for the concept of the characteristic earthquake model itself.

[92] Table 7 shows that in general the computed Coulomb stress change is variable over the geographical extension of the concerned fault, and in many cases it ranges from negative to positive values, due to its spatial variability with respect to the source dimensions. This circumstance makes it difficult to predict the effect of the stress change on the next occurrence time, as we don't have an idea of the future nucleation point. In this circumstance we have considered the minimum, mean and maximum ΔCFF, as well as the minimum, mean and maximum clock advance Δt.

[93] It is interesting to note also that, even taking the maximum clock advance as a conservative measure, only for one source the stress change due to the subsequent events has significantly affected the estimated probability of occurrence, increasing its value. This is the case of Ovindoli-Pezza for which the probability has increased from 1.5% (column 5 of Table 6) to 2.8% (column 8 of Table 8). For other sources, the change was less important. Among these cases, we can notice Monte Sant'Angelo (from 4.2% to 4.7%, column 5 of Table 6 and column 8 of Table 8, respectively) and Sulmona (from 6.2% to 6.6%, column 5 of Table 6 and column 8 of Table 8, respectively).

[94] Looking at Table 9, the last column of which reports the hazard rate computed at the present time, taking into account the transient effect of the Coulomb stress change, it can be noted that this effect does not have influence on the hazard estimate. This is easily explained by the fact that the most important events that could have produced such transient effect are dated centuries ago. Even the most recent failures (those breaking the ITGG053 and ITGG054 sources) occurred in October–November 2002 that is about 5 years before the date of computation (1 January 2007), the transient effect is negligible. During this time the rate modeled by the decay law of equation (9), similar to the Omori law, might have nearly returned back to its background value.

5.2. Uncertainty Analysis

[95] The overall methodology appears affected by large uncertainties on several of its key points. The largest factors that contribute to such uncertainties come from:

[96] 1. The recurrence times adopted in the renewal model;

[97] 2. The value of the coefficient of variation;

[98] 3. The stress rate on the seismogenic structures obtained from geodetic information;

[99] 4. The value of the Coulomb stress change computed through the elastostatic model, approximating the causative fault to a rectangular shape with uniform stress drop, and its variability across the triggered fault;

[100] 5. The date of the latest characteristic earthquake, for some sources the historical information of which is lacking.

[101] Moreover, other factors of uncertainty should also be taken into account. Among them the uncertainty affecting source parameters (strike, slip and rake) and the friction coefficient.

Table 9. Mean Hazard Rate on the Seismogenic Faults Computed as of 1 January 2007 Under the Four Models

Source Code	Source Name	Poisson	Conditional BPT	Permanent Effect Modified by ΔCFF	Transient Effect Modified by ΔCFF
ITGG001	Ovindoli-Pezza	3.89e − 04	2.83e − 04	3.76e − 04	3.76e − 04
ITGG002	Fucino Basin	5.26e − 04	0.00e + 00	1.78e − 03	1.17e − 04
ITGG003	Aremogna-Cinque Miglia	3.41e − 04	6.56e − 04	4.43e − 04	4.43e − 04
ITGG004	Boiano Basin	1.42e − 04	0.00e + 00	2.82e − 04	2.82e − 04
ITGG005	Tammaro Basin	1.47e − 04	0.00e + 00	7.37e − 04	7.37e − 04
ITGG006	Ufita Valley	1.62e − 04	0.00e + 00	6.17e − 04	6.17e − 04
ITGG008	Agri Valley	1.78e − 04	0.00e + 00	3.82e − 04	3.82e − 04
ITGG010	Melandro-Pergola	1.87e − 04	0.00e + 00	8.21e − 04	8.21e − 04
ITGG015	Montereale Basin	3.83e − 04	0.00e + 00	8.16e − 04	8.16e − 04
ITGG016	Norcia Basin	4.57e − 04	0.00e + 00	4.04e − 04	4.04e − 04
ITGG019	Sellano	4.76e − 04	0.00e + 00	8.38e − 06	8.38e − 06
ITGG020	Monte Sant'Angelo	7.46e − 04	8.23e − 04	1.22e − 03	1.22e − 03
ITGG022	San Marco Lamis	2.08e − 04	0.00e + 00	3.19e − 04	3.19e − 04
ITGG026	Amatrice	5.12e − 04	4.63e − 06	3.27e − 04	3.27e − 04
ITGG027	Sulmona Basin	9.09e − 04	1.23e-03	7.19e − 04	7.19e − 04
ITGG028	Barrea	3.82e − 04	0.00e + 00	2.54e − 05	2.54e − 05
ITGG052	San Giuliano di Puglia	5.00e − 04	0.00e + 00	4.72e − 06	4.72e − 06
ITGG053	Ripabottoni	5.56e − 04	0.00e + 00	4.72e − 06	4.72e − 06
ITGG054	San Severo	1.44e − 04	0.00e + 00	4.80e − 04	4.80e − 04
ITGG061	Foligno	3.45e − 04	0.00e + 00	4.72e − 04	4.72e − 04
ITGG062	Trevi	3.47e − 04	0.00e + 00	3.35e − 04	3.35e − 04
ITGG070	Offida	2.50e − 04	0.00e + 00	3.49e − 04	3.49e − 04
ITGG077	Colliano	3.33e − 04	0.00e + 00	0.00e + 00	0.00e + 00
ITGG078	San Gregorio Magno	3.18e − 04	0.00e + 00	0.00e + 00	0.00e + 00
ITGG079	Pescopagano	3.18e − 04	0.00e + 00	0.00e + 00	0.00e + 00
ITGG080	Cerignola	1.67e − 04	0.00e + 00	2.78e − 04	2.78e − 04
ITGG081	Melfi	1.52e − 04	0.00e + 00	2.92e − 04	2.92e − 04
ITGG082	Ascoli Satriano	2.38e − 04	0.00e + 00	1.00e − 03	1.00e − 03
ITGG083	Bisceglie	3.45e − 04	0.00e + 00	9.78e − 04	9.78e − 04
ITGG084	Potenza	3.85e − 04	0.00e + 00	7.94e − 04	7.94e − 04
ITGG088	Bisaccia	1.05e − 04	0.00e + 00	8.58e − 04	8.58e − 04
ITGG092	Ariano Irpino	5.00e − 05	0.00e + 00	4.63e − 04	4.63e − 04
ITGG094	Tocco da Casauria	2.22e − 04	0.00e + 00	1.04e − 03	1.04e − 03
ITGG095	Frosolone	5.33e − 05	0.00e + 00	1.20e − 04	1.20e − 04
ITGG096	Isola del Gran Sasso	4.00e − 04	0.00e + 00	1.30e − 04	1.30e − 04

[102] To get an idea of the effect of the compounded uncertainty from all of the above mentioned factors, we have applied a decision tree approach to the problem. There are eight uncertainty factors. If we consider for each of them the minimum and maximum value for each parameter according to its assumed uncertainty, this gives 256 possible combinations. We have developed a computer code for computing the 50 years probability of occurrence for all the 256 combinations of uncertainties. Figure 3 gives a sketch of our decision tree.

[103] For each of the 35 individual sources we obtain a distribution for the 256 values of the probability of failure for the next 50 years. Figure 4 shows a typical histogram of this distribution for the source ITGG037 (Sulmona Basin).

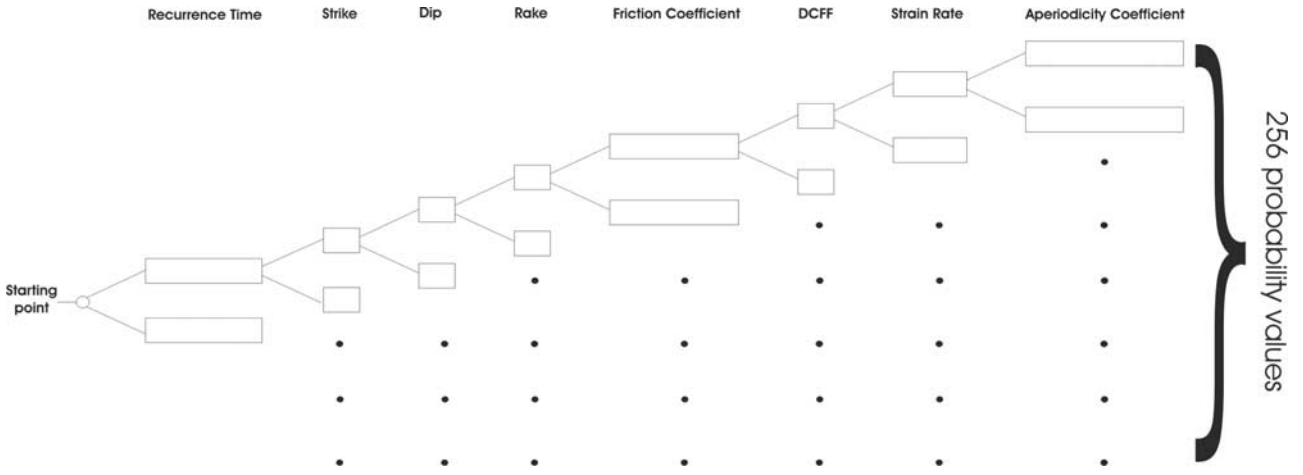

Figure 3. Logical tree for the calculation of probabilities of failure in the next 50 years for the sources considered in this study. The 256 solutions for each source are obtained by variations of the 8 model parameters: recurrence time, strike, dip, rake, friction coefficient, Coulomb Failure Function (ΔCFF), strain rate, aperiodicity coefficient.

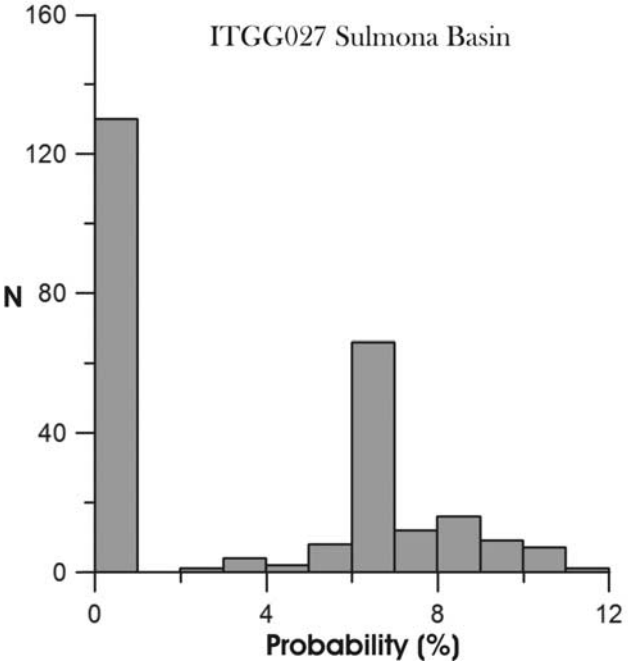

Figure 4. Distribution of the 256 probability values for the seismogenic source of Sulmona Basin.

As for many other cases, this distribution is bimodal, with a peak at 0% and another peak at some values around a few %. This peak at higher probability values is probably related to the minimum values of the recurrence time and/or the largest aperiodicity.

[104] For each of the 35 sources, we have estimated the 10, 50 and 90 percentile of the respective probability distribution. The results are shown in Figure 5, In the same figure, for sake of comparison, we have also represented, for each source, the probabilities obtained from the Poisson model and the mean of the BPT renewal model. The 90 percentiles are, in 28 cases out of 35, larger than the Poisson estimates, while the 10 and 50 percentiles are systematically smaller. This is due to the large proportion of zero values over each set of 256 probability samples for the renewal model. The mean probabilities obtained from the average of each set are of the same order of magnitude of, but more often larger than the Poisson probabilities for the same source. This is related with the extreme asymmetry of the probability distributions.

6. Conclusions

[105] We have applied a renewal model based on the BPT distribution, including the permanent and transient effect of the stress interaction among faults, to 35 seismogenic faults of the Southern Apennines in Italy, that are described in the DISS 3.0.2 database. The recurrence times reported in this

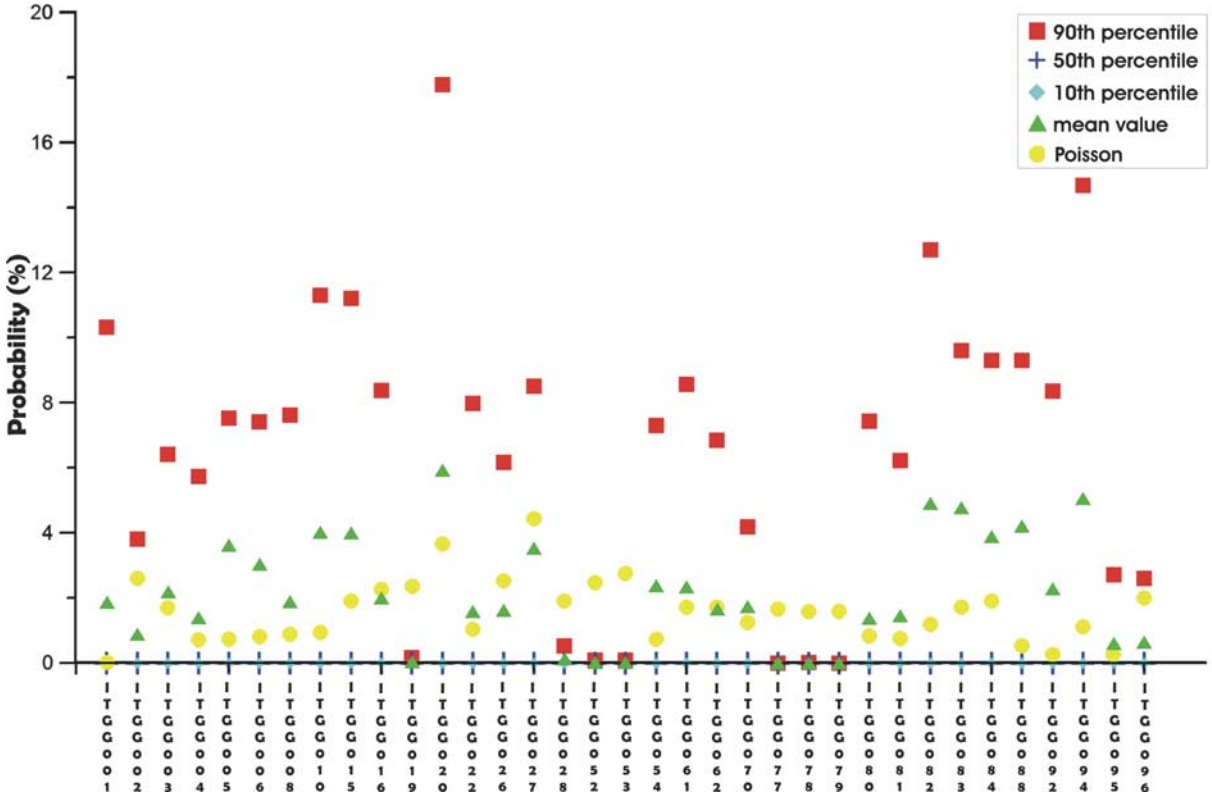

Figure 5. Occurrence probability of failures for the main earthquake sources in the next 50 years in Southern Italy, based on a Poisson time-independent model (yellow points) and on a renewal BPT time-dependent model for a 10th (blue cross), 50th (blue diamond), 90th percentile (red square) and mean value (green triangle).

database, jointly with the values obtained from geodetic observations, range typically from 2,000 to 10,000 years.

[106] According to the results of our analysis, the number of large earthquakes occurred during the latest hundreds years in Italy has been much larger than would have been expected from the methodology adopted in this study. Besides the hypothesis that the latest centuries might have been anomalously active, this circumstance can be explained in three ways: (1) the recurrence times are strongly overestimated, or (2) there are many more sources, still unknown because they have not ruptured in the latest few centuries, that are missing in the database, or (3) the application of the characteristic earthquake model to the Italian seismicity is questionable. Any of these three cases has large impact on seismic hazard assessment in Italy.

[107] The most important conclusion that can be drawn from our study is that the renewal model predicts probabilities of failure of these faults for the next 50 years that are substantially lower than those based on the Poisson time-independent model. This result is easily explained by the fact that the time elapsed since the latest characteristic earthquake is shorter than the estimated recurrence time for most of the sources examined in this study. The permanent effect of the stress change doesn't affect very much the conditional probability obtained from the unperturbed model, and the transient effect, modeling a sort of aftershock rate decay, has also a minor role after more than 5 years since the latest event reported in the database, the San Giuliano di Puglia, 2002 earthquake.

[108] A comparison between the recurrence times inferred from the analysis carried out on five faults for which paleoseismological information was available, and those obtained through the geodetic slip rate has shown relevant discrepancies between these results. The paleoseismological data are, in our study, the only source of information concerning the coefficient of variation, or aperiodicity, for modeling the inter-event time distribution by a renewal process such as the BPT distribution. For only two sources of five, this analysis has given some evidence of an aperiodicity value significantly smaller than 1.0.

[109] An application of the decision tree approach has shown a wide variability of the probability of failure for all the characteristic sources in the next 50 years. While the 10th and 50th percentiles of these probabilities are generally zero, the 90th percentiles go up to even more than 10%.

[110] We reach the conclusion that the present status of both the methodology and the quality of input data for time-dependent earthquake hazard assessment in Southern Italy are still at a premature stage for drawing results that can reliably substitute the time-independent Poisson hypothesis based on the Gutenberg-Richter relationship.

Appendix A

[111] Assuming that the stress drop of a characteristic earthquake is a known constant parameter, we want to obtain the average slip $\overline{\Delta u}$ for an earthquake of given size. The scalar seismic moment of an earthquake is defined as

$$M_0 = \mu \overline{\Delta u} S, \tag{A1}$$

where μ is the shear modulus of the elastic medium, S is the area of the fault, that for a rectangular shape is the product of the length L by the width W. An approximate formula for the seismic moment versus the stress drop $\Delta\sigma$ for a rectangular fault is [*Console and Catalli*, 2007]:

$$M_0 = \frac{\pi^2}{32} \Delta\sigma (WL)^{3/2}, \tag{A2}$$

and eliminating the seismic moment from equations (A1) and (A2), we obtain:

$$\overline{\Delta u} = \frac{\pi^2}{32} \frac{\Delta\sigma}{\mu} (WL)^{1/2}. \tag{A3}$$

This equation shows that the average slip is proportional to the stress drop for the same area of the fault, and allows the computation of the expected average slip from the size of the fault.

[112] A reasonable value for the stress drop $\Delta\sigma$ can be inferred in the following way. The physics of fractures in elastic media leads to a theoretical relationship between the scalar seismic moment M_0 and the energy E_s released by an earthquake through seismic waves:

$$\frac{E_s}{M_0} = \frac{\overline{\Delta\sigma}}{2\mu}, \tag{A4}$$

where $\overline{\Delta\sigma}$ is the average stress drop.

[113] Two widely used formulas link the seismic moment and the seismic energy of an earthquake with the magnitude:

$$\log E_s(joule) = 4.8 + 1.5M \tag{A5}$$

[*Gutenberg and Richter*, 1956] and

$$\log M_0(N \cdot m) = 9.1 + 1.5M. \tag{A6}$$

[*Hanks and Kanamori*, 1979].

[114] By substitution of E_s and M_0 from equations (A5) and (A6) into equation (A4), we easily obtain:

$$\overline{\Delta\sigma} = \frac{2\mu}{10^{4.3}} \cong \mu \cdot 10^{-4}, \tag{A7}$$

that, adopting the usual value $\mu = 3 \cdot 10^{10}$ Pa for rocks in the Earth crust, gives

$$\overline{\Delta\sigma} \cong 3 \cdot 10^6\ Pa. \tag{A8}$$

[115] If we want to compute the slip rate $\frac{d\Delta u}{dt}$ on a fault of given size, starting from the strain rate $\dot{\varepsilon}$ obtained from geodetic observations, we may still make use of equation (A3), by deriving it with respect to time, in the following way:

$$\frac{d\Delta u}{dt} = \frac{\pi^2}{32} \frac{\dot{\tau}}{\mu} (WL)^{1/2} = \frac{\pi^2}{32} \dot{\varepsilon} (WL)^{1/2}. \tag{A9}$$

[116] **Acknowledgments.** We thank Tom Parsons and an anonymous reviewer for their useful comments that contributed to a significant improvement of the article. This work was partially supported for the years 2005–2007 by grants from the Italian Department for Civil Protection (DPC) and the Istituto Nazionale di Geofisica e Vulcanologia (INGV) in the frame of project S2 "Evaluation of potential seismogenic and probability of large earthquakes in Italy" – Task 4 "Characterizing the behavior of seismogenic sources and assigning probabilities of activation," in the object UR 4.7 "Occurrence probability of moderate and large events, using dataset of instrumental and historical events".

References

Basili, R., G. Valensise, P. Vannoli, P. Burrato, U. Fracassi, S. Mariano, M. M. Tiberti, and E. Boschi (2008), The Database of Individual Seismogenic Sources (DISS), version 3: Summarizing 20 years of research on Italy's earthquake geology, *Tectonophysics*, doi:10.1016/j.tecto.2007.04.014.

Boschi, E., P. Gasperini, and F. Mulargia (1995), Forecasing where larger crustal earthquakes are likely to occur in Italy in near future, *Bull. Seismol. Soc. Am.*, *85*(5), 1475–1482.

Console, R., and F. Catalli (2007), A rate-state model for aftershocks triggered by dislocation on a rectangular fault: A review and new insights, *Ann. Geophys.*, *49*(6), 1259–1273.

Console, R., M. Murru, and F. Catalli (2006), Physical and stochastic models of earthquake clustering, *Tectonophysics*, *417*, 141–153.

Console, R., M. Murru, F. Catalli, and G. Falcone (2007), Real time forecasts through an earthquake clustering model constrained by the rate-and-state constitutive law: Comparison with a purely stochastic ETAS model, *Seism. Res. Lett.*, *78*(1), 49–56.

CPTI04 (2004), *Parametric Catalog of the Italian Earthquakes*, Istituto Nazionale di Geofisica e Vulcanologia, Rome. (Available at http://emidius.mi.ingv.it/CPTI04/)

CSI (2007), *Catalog of the Italian Seismicity*, Istituto Nazionale di Geofisica e Vulcanologia, Rome. (Available at http://ingv.it/CSI/)

Dieterich, J. H. (1986), A model for the nucleation of earthquake slip, in *Earthquake Source Mechanics*, *Geophys. Monog.*, *37*, 36–49, Maurice Ewing Series, AGU, Washington, D. C.

Dieterich, J. H. (1992), Earthquake nucleation on faults with rate and state dependent strength, *Tectonophysics*, *211*, 115–134.

Dieterich, J. H. (1994), A constitutive law for rate of earthquake production and its application to earthquake clustering, *J. Geophys. Res.*, *99*, 2601–2618.

DISS Working Group (2006), Database of Individual Seismogenic Sources (DISS), Version 3.0.2: A compilation of potential sources for earthquakes larger than M 5.5 in Italy and surrounding areas, Istituto Nazionale di Geofisica e Vulcanologia 2005, Rome. (Available at http://www.ingv.it/DISS/)

Ellsworth, W. L., M. V. Matthews, R. M. Nadeau, S. P. Nishenko, and P. A. Reasenberg (1999), A physically based recurrence model for estimation of long-term earthquake probabilities, *US Geol. Surv. Open-File Rep.*, 99–522.

Fedotov, S. A. (1968), The seismic cycle, quantitative seismic zoning, and long-term seismic forecasting, in *Seismic Zoning in the USSR*, edited by S. V. Medvev, pp. 133–166, Izdatel'stvo Nauka, Moscow.

Field, E. H., D. D. Jackson, and J. F. Dolan (1999), A mutually consistent seismic-hazard source model for Southern California, *Bull. Seismol. Am.*, *89*(3), 559–578.

Gomberg, J., P. Reasenberg, N. Beeler, M. Cocco, and M. E. Belardinelli (2005a), A frictional population model of seismicity rate change, *J. Geophys. Res.*, *110*, B05S03, doi:10.1029/2004JB003404.

Gomberg, J., P. Reasenberg, N. Beeler, M. Cocco, and M. E. Belardinelli (2005b), Time-dependent earthquake probabilities based on population models, *J. Geophys. Res.*, *110*, B05S04, doi:10.1029/2004JB003405.

Gutenberg, B., and C. F. Richter (1956), Earthquake magnitude, intensity, energy and acceleration, *Bull. Seismol. Soc. Am.*, *46*, 105–145.

Hagiwara, Y. (1974), Probability of earthquake occurrence as obtained from a Weibull distribution analysis of crustal strain, *Tectonophysics*, *23*, 318–323.

Hanks, T. C., and H. Kanamori (1979), A moment magnitude scale, *J. Geophys. Res.*, *84*(B5), 18,025–18,028.

Harris, R. A., and R. W. Simpson (1998), Suppression of large earthquakes by stress shadows: A comparison of Coulomb and rate-and-state failure, *J. Geophys. Res.*, *103*, 24,439–24,451.

Kagan, Y. Y., and L. Knopoff (1987), Random stress and earthquake statistics: Time dependence, *Geophys. J. R. Astron. Soc.*, *88*, 723–731.

King, G. C. P., and M. Cocco (2001), Fault interaction by elastic stress changes: New clues from earthquake sequences, *Adv. Geophys.*, *44*, 1–39.

King, G. C. P., R. S. Stein, and J. Lin (1994), Static stress changes and the triggering of earthquakes, *Bull. Seismol. Soc. Am.*, *84*, 935–953.

Matthews, M. V., W. L. Ellsworth, and P. A. Reasenberg (2002), A Brownian model for recurrent earthquakes, *Bull. Seismol. Soc. Am.*, *92*, 2233–2250.

Mc Cann, W. R., S. P. Nishenko, L. R. Sykes, and J. Krause (1979), Seismic gaps and plate tectonics: Seismic potential for maior boundaries, *Pure Appl. Geophys.*, *117*, 1082–1147.

Murru, M., R. Console, and A. Lisi (2004), Seismicity and mean magnitude variations correlated to the strongest earthquakes of the 1997 Umbria-Marche sequence (Central Italy), *J. Geophys. Res.*, *109*, B01304, doi:10.1029/2002JB002276.

Nishenko, S. P. (1989), Earthquakes: Hazards and prediction, in *The Encyclopedia of Solid Earth Geophysics*, edited by D. E. James, pp. 260–268, Van Nostrand Reinhold, New York.

Nishenko, S. P. (1991), Circum-Pacific potential–1989–1999, *Pure. Appl. Geophys.*, *198*, 169–259.

Nostro, C., L. Chiaraluce, M. Cocco, D. Baumont, and O. Scotti (2005), Coulomb stress changes caused by repeated normal faulting earthquakes during the 1997 Umbria-Marche (central Italy) seismic sequence, *J. Geophys. Res.*, *110*, B05S20, doi:10.1029/2004JB003386.

Pace, B., L. Peruzza, G. La Vecchia, and P. Boncio (2006), Layered seismogenic source model and probabilistic seismic-hazard analyses in Central Italy, *Bull. Seismol. Soc. Am.*, *96*, 107–132.

Pantosti, D. (2000), Earthquake recurrence through time, in *Proceeding of the Hokudan International Symposium and School on Active Faulting*, Hokuda Co. Ltd., Awaji Island, Hyogo, Japan, 17th–26th January 2000, pp. 363–365.

Pantosti, D., D. P. Schwartz, and G. Valensise (1993), Paleoseismicity along the 1980 surface rupture of the Irpinia fault: Implications for earthquake recurrence in Southern Apennines, Italy, *J. Geophys. Res.*, *98*, 6561–6577.

Parsons, T. (2004), Recalculated probability of $M \geq 7$ earthquakes beneath the Sea of Marmara, Turkey, *J. Geophys. Res.*, *109*, B05304, doi:10.1029/2003JB002667.

Parsons, T. (2005), Significance of stress transfer in time-dependent earthquake probability calculations, *J. Geophys. Res.*, *109*, B05304, doi:10.1029/2003JB002667.

Parsons, T. (2008), Monte Carlo method for determining earthquake recurrence parameters from short paleoseismic catalogs: Example calculations, *J. Geophys. Res.*, *113*, B03302, doi:10.1029/2007JB004998.

Rhoades, D. A., and R. J. Van Dissen (2003), Estimates of the time-varying hazard of rupture of the Alpine Fault, New Zealand, allowing for uncertainties, *N. Z. J. Geol. Geophys.*, *46*, 479–488.

Rhoades, D. A., R. J. Van Dissen, and D. J. Dowrick (1994), On the handling of uncertainties in estimating the hazard of rupture on a fault segment, *J. Geophys. Res.*, *99*(B7), 13,701–13,712.

Rikitake, T. (1974), Probability of an earthquake occurrence as estimated from crustal strain, *Tectonophysics*, *23*, 299–312.

Ruina, A. (1983), Slip instability and state variable friction laws, *J. Geophys. Res.*, *88*(B12), 10,359–10,370.

Schwartz, D. P., and K. J. Coppersmith (1984), Fault behavior and characteristic earthquakes: Examples from Wasatch and San Andreas fault zones, *J. Geophys. Res.*, *89*, 5681–5698.

Serpelloni, E., M. Anzidei, P. Baldi, G. Casula, and A. Galvani (2005), Crustal velocity and strain-rate fields in Italy and surrounding regions: New results from the analysis of permanent and non-permanent GPS networks, *Geophys. J. Int.*, *161*, 861–880.

Shimazaki, K., and T. Nakata (1980), Time-predictable recurrence model for large earthquakes, *Geophys. Res. Lett.*, *7*, 279–282.

Stein, R., A. Barka, and J. Dieterich (1997), Progressive failure on the North Anatolian fault since 1939 by earthquake stress triggering, *Geophys. J. Int.*, *128*, 594–604.

Toda, S., R. Stein, P. Reasenberg, J. Dieterich, and A. Yoshida (1998), Stress transferred by the 1995 Mw = 6.9 Kobe, Japan, shock: Effect on aftershocks and future earthquake probabilities, *J. Geophys. Res.*, *103*(B10), 24,543–24,565.

Utsu, T. (1972a), Large earthquakes near Hokkaido and the expectancy of the occurrence of a large earthquake of Nemuro, *Rep. Coord. Comm. Earthquake Predict.*, *7*, 7–13.

Utsu, T. (1972b), Aftershocks and earthquake statistics (IV), *J. Fac. Sci., Hokkaido Univ., Ser. 7*, *4*, 1–42.

Wells, D. L., and K. J. Coppersmith (1994), New empirical relationships among magnitude, rupture length, rupture width, rupture area, and surface displacement, *Bull. Seismol. Soc. Am.*, *84*(4), 974–1002.

Zöller, G., and S. Hainzl (2007), Recurrence time distributions of large earthquakes in a stochastic model for cupled fault systems: The role of fault interaction, *Bull. Seismol. Soc. Am.*, *97*(5), 1679–1687.

F. Catalli, R. Console, G. Falcone, and M. Murru, Istituto Nazionale di Geofisica e Vulcanologia, Via di Vigna Murata, 605 00143 Rome, Italy. (console@ingv.it)